Electronic Research Archive

https://www.aimspress.com/journal/era

ERA, 32(12): 6733–6760.
DOI: 10.3934/era.2024315
Received: 12 September 2024
Revised: 23 November 2024
Accepted: 04 December 2024
Published: 16 December 2024

Research article

An application of potential function in robot path planning and three optimized formulas for equivalent resistance

Jianwei Dai[1], **Xiaoyu Jiang**[1,*], **Yanpeng Zheng**[2,*], **Xing Zhang**[1] **and Zhaolin Jiang**[3]

[1] School of Information Science and Engineering, Linyi University, Linyi 276000, China
[2] School of Automation and Electrical Engineering, Linyi University, Linyi 276000, China
[3] School of Mathematics and Statistics, Linyi University, Linyi 276000, China

* **Correspondence:** Email: jxy19890422@sina.com, zhengyanpeng0702@sina.com.

Abstract: The study proposed an innovative path planning algorithm based on the potential function of a special case of the cobweb resistor network, addressing the path planning problem in globe environments with obstacles. For the non-regular $m \times n$ cobweb resistor network with arbitrary longitude, we found that by introducing Chebyshev polynomial of the second class, the precise equivalent resistance formulas could be optimized effectively. Compared with the original formula, optimized equivalent resistance formulas significantly reduced the time cost in large-scale data calculations. Furthermore, we have plotted 3D views of the equivalent resistance formulas for several special cases and conducted simulation experiments on the computational efficiency of the original and optimized formulas at different data scales, verifying the superiority of the optimized formulas. These findings provided new perspectives and tools for the computation of resistor networks and the design of path planning algorithms.

Keywords: resistor network; potential function; path planning; Chebyshev polynomial; equivalent resistance

1. Introduction

Tan [1] innovatively constructed a mathematical model of the non-regular cobweb resistor network with arbitrary longitude. Through analyzing this model, an extremely precise equivalent resistance function was obtained theoretically. This groundbreaking work has significant implications for multiple fields. As is well-known, the most common way of analyzing and solving problems in classical physics is to build physical mathematical models. The large-scale numerical computation of physical models has been replaced by computers, which holds profound implications for traditional science and engineering. In addition, researchers are well aware that improving the computational efficiency

of equivalent resistance is of utmost importance for the progress and development of related fields. Therefore, to better adapt to computer analysis, optimizing the equivalent resistance formula is a good choice. In this paper, we re-expressed the original function using Chebyshev polynomial of the second class, resulting in greatly improved computational efficiency.

The rapid pace of advancement in modern scientific development exceeds imagination, yet the complex challenges faced across various fields cannot be overlooked. A large amount of research shows that resistor network models [2–7] can well address a considerable part of the complex challenges. By using the resistor network model, it is possible to quantify the low conductivity areas in organic thin films [2], analyze and design the grating of general printed circuit boards [3], simulate the interaction of magnetic fields [4], establish nonlinear circuit arrays for self-induced topological protection [5], locate the damage in materials [6], perform 3D modeling of the conductivity of materials [7], etc.

Path planning problems have always attracted the attention of researchers, and the research results related to path planning have been widely applied [8–11]. Among them, the most challenging problem is path planning on special spatial shapes which has been researched in recent years [12–15]. This paper employs resistor networks as a tool to tentatively propose a new robot path planning algorithm. This scheme is based on the heuristic algorithm of potential function and incorporates a unique cobweb model. This will undoubtedly provide a broader perspective for related research in path planning.

This paper is structured as follows: In Section 2, we introduce some of the development history of resistor networks. In Section 3, we discuss the path planning algorithm designed for the globe environment based on the potential function. Section 4 presents the original exact equivalent resistance formulas for the cobweb resistor network. In Section 5, we describe the optimized exact equivalent resistance formulas. Section 6 details the derivation process of the optimized formulas. Section 7 provides 3D views of the equivalent resistance formulas under several special conditions. In Section 8, we compare the computational efficiency of the original and optimized formulas through specific experiments.

2. Background

Since the introduction of Kirchhoff's laws [16], the development of resistor networks has been continuous. However, progress has been significantly slowed by the complexities of boundary conditions. Infinite resistor networks do not require consideration of boundary conditions; hence, researchers have initially studied infinite resistor networks using methods such as electromigration [17], Poisson equation [18], impedance theory [19–22], graph theory [23–27], Green's functions [28–31] and some special methods [32–34]. The research on finite resistor networks has progressed relatively slowly, until 2004 when Wu [35] proposed the Laplacian matrix (LM) method and achieved some relevant research results [35–39]. However, the LM method is only applicable to resistor networks with regular boundaries.

To achieve a new theoretical breakthrough, Tan proposed the recursive transformation (RT) method. Compared to the LM method, the RT method is better suited for handling resistor networks with complex boundary conditions. In 2014, Tan et al. [40] first solved the resistance formula for globe resistor networks. Te RT methods includes the RT-V method based on node voltage and the RT-I method based on branch current. Subsequently, Tan et al. studied other three-dimensional resistive network models using the RT-V method [41–46] and RT-I method [47, 48], respectively. The contributions of Tan et al.

to the field of resistor networks are undeniable. It is worth noting that the utilization of the RT method involves many aspects related to tridiagonal matrices. The tridiagonal matrices have yielded numerous reliable conclusions [49–55]. It is interesting that the inverses of some special Toeplitz matrices are also the perturbed tridiagonal Toeplitz matrices [56–59]. In recent years, Shi et al. [60–66] made achievements in the field of neural networks that has also provided certain inspirations for the study of resistor networks. Some researchers in the field of resistor networks have begun to apply various methods to improve computational efficiency in solving resistor network models [67–70], further advancing the development of the resistor network domain.

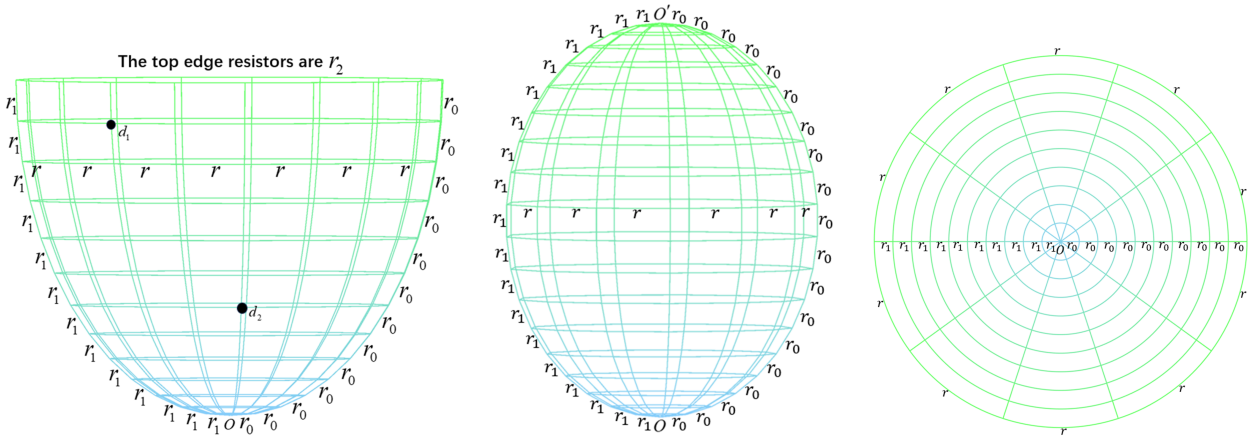

Figure 1. **(a)** is a non-regular $m \times n$ cobweb with an arbitrary top boundary and longitude (with r_1), which has m latitudes and n longitudes. Excluding the resistance r_1 on one specific longitude and the resistance r_2 at the top, the resistances in the longitudinal and latitudinal directions are r_0 and r, respectively; **(b)** is a $m \times n$ globe network with an arbitrary longitude, which has m latitudes and n longitudes. Bonds in the longitudes and latitudes directions represent, respectively, resistors r_0 and r except for the resistance r_1 on one arbitrary longitude; **(c)** is an $m \times n$ conventional cobweb network with an arbitrary longitude, which has m latitudes and n longitudes. Bonds in the longitudes and latitudes directions represent, respectively, resistors r_0 and r except for the resistance r_1 on one arbitrary longitude.

3. An application of potential function in path planning

In this section, we will design a preliminary path planning method suitable for the globe Figure 1(b) model as an example.

3.1. Potential function

In 2018, Tan et al. [43] first used the recursion transformation method with current parameters (RT-I) to derive the accurate potential function of the globe resistor network. In 2022, Zhou et al. [68] optimized the potential function of the globe resistor network. The optimized potential function is as follows

$$\frac{U_{m\times n}(x,y)}{J} = \frac{y(y_1-y_2)}{mn}r_0 + \frac{2r}{m}\sum_{j=2}^{m}\frac{\gamma_{x_1,x}^{(j)}C_{y_1,j} - \gamma_{x_2,x}^{(j)}C_{y_2,j}}{t_j U_{n-1}^{(j)} - 2U_{n-2}^{(j)} - 2}C_{y,j}, \tag{3.1}$$

where

$$\gamma^{(j)}_{x_s,x_k} = U^{(j)}_{n-|x_s-x_k|-1} + U^{(j)}_{|x_s-x_k|-1}, \quad s = 1,\ 2, \tag{3.2}$$

$$C_{p,j} = \sin(\frac{p(j-1)\pi}{m}), \quad p = y_1,\ y_2,\ y, \tag{3.3}$$

$$t_j = 2 + \frac{2r}{r_0} - \frac{2r}{r_0}\cos\frac{(j-1)\pi}{m}, \tag{3.4}$$

$$U^{(j)}_k = U^{(j)}_k(\cos\psi_j) = \frac{\sin(k+1)\psi_j}{\sin(\psi_j)}, \quad \psi_j = \arccos\left(1 + \frac{r}{r_0} - \frac{r}{r_0}\cos\frac{(j-1)\pi}{m}\right), \tag{3.5}$$

$$k = n - |x_1 - x|,\ |x_1 - x|,\ n - |x_2 - x|,\ |x_2 - x|,\ n-1,\ n-2,\ j = 1,\ 2, \ldots,\ m.$$

3.2. Path planning algorithm

This method (the potential function path planning method) completes the robot path planning by simulating the potential drop from the current input point to the output point. Compared with the traditional artificial potential field method, this method is more suitable for robot path planning of the globe model and can better adapt to the cyclic characteristics of the model's latitude direction. The description of the related robot path planning algorithm is as follows:

Step 1: Set the robot's work environment map, including the starting and ending points, and obstacle locations, based on the grid method.

Step 2: Assign the starting point and the target point to the input and output points of the current in the globe resistor network, respectively, and use the potential formula (3.1) to calculate the potential.

Step 3: Increase a fixed amount of potential at the corresponding nodes in the globe resistor network where the grid points of the obstacles are located. The potential after the fixed increment is added in $\frac{U(x,y)}{J} + 0.3\frac{U(x_1,y_1)}{J}$, where the $\frac{U(x_1,y_1)}{J}$ denotes the potential at the starting point.

Step 4: Use $\min\left\{\frac{U(x+i,y+j)}{J}\right\}(\{(i,j)\,|i,j \in \{-1,0,1\}, (i,j) \neq (0,0)\})$ to select the node with the smallest potential adjacent to the robot.

Step 5: Move the robot to the grid point corresponding to the node selected in Step 4 and update its current position.

Step 6: Determine whether the current position of the robot is the target point. If it is, terminate the algorithm. Otherwise, repeat Step 4.

Step 7: End the algorithm.

3.3. Detailed explanation of path planning method

To enhance the visual clarity of the results produced by our path planning method. Let $m = n = 10,\ x_1 = 7,\ y_1 = 8,\ x_2 = 3,\ y_2 = 2,\ r = 1,\ r_0 = 1$, and $J = 1$, where (x_1, y_1) and (x_2, y_2) correspond to the starting point and ending point of the robot in path planning respectively.

The overall approach of our designed path planning method is very clear. First, based on the actual globe environment containing obstacles, we grid the globe environment, placing obstacles at the grid nodes. Next, we construct a resistor network corresponding to the shape of the physical grid, which does not include obstacles. Then, we solve for the node potentials using formula (3.1) and plot the distribution of the potentials across all nodes in the resistor network. Subsequently, we plot the potential distribution map, where the potentials at the nodes corresponding to the obstacles are weighted. Using this weighted potential distribution map, we apply the gradient descent method to determine the

optimal path for the robot. Finally, we map the optimal path obtained from the above process onto the actual globe environment map containing obstacles. The implementation process of the overall idea of path planning is shown from Figure 2 to Figure 4.

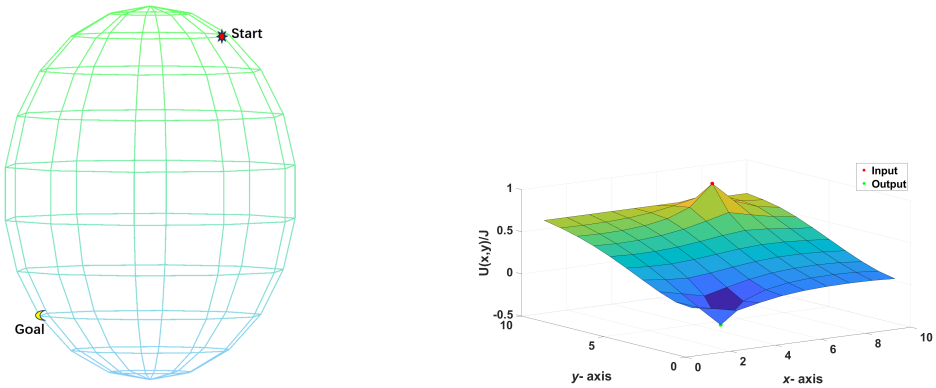

(a) **(b)**

Figure 2. **(a)** Globe environment map without obstacles; **(b)** Potential distribution diagram of a globe resistor network.

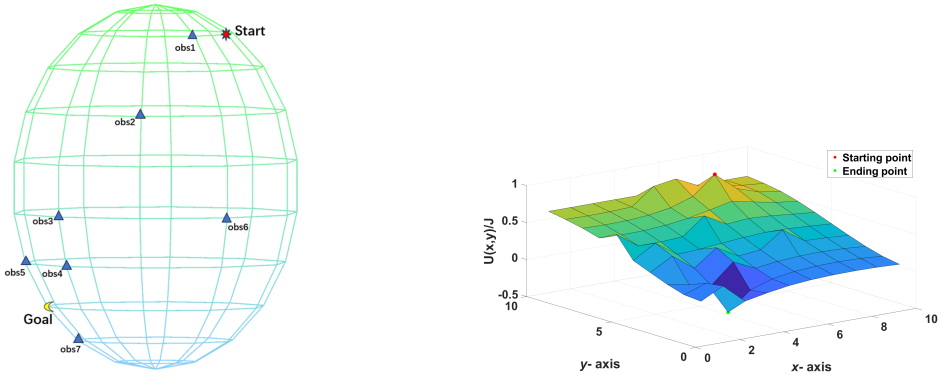

(a) **(b)**

Figure 3. **(a)** Globe environment map after adding obstacles; **(b)** Potential distribution diagram after node-weighted adjustments for obstacles.

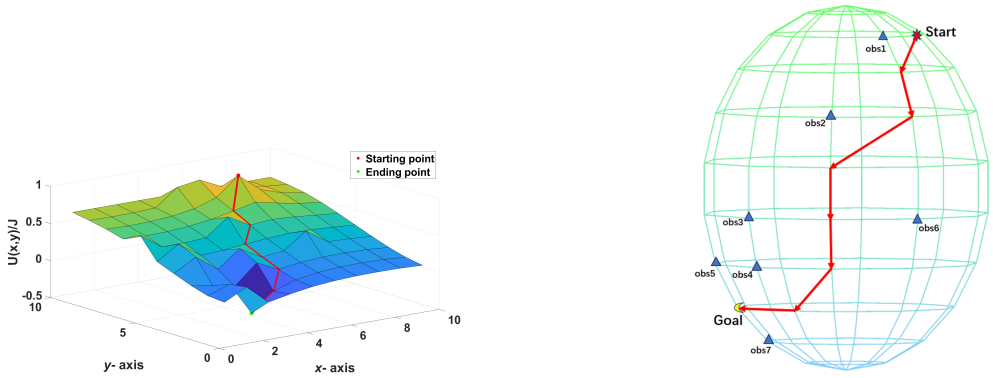

(a) **(b)**

Figure 4. **(a)** Path planning in node-weighted potential distribution diagram; **(b)** Path planning in the globe environment map.

In the future, we will further study the path planning problem on the globe network, and we also hope that this method can provide help to related researchers.

4. The original formulas for equivalent resistance between any two points

In 2015, Tan [1] used the RT-I method for the first time to study a non-regular cobweb network as shown in Figure 1(a). We have derived the general formula for the equivalent resistance when $r_2 = \{0,\ r,\ 2r\}$. When $r_2 = 0$, the cobweb network transforms into the globe network, as shown in Figure 1(b). The equivalent resistance between any two nodes $d_1\,(x_1, y_1)$ and $d_2\,(x_2, y_2)$ in a nearly $m \times n$ cobweb network with 0 boundary is

$$R_{m\times n}(d_1, d_2) = \frac{r_0 r_1 (y_2 - y_1)^2}{m\left[(n-1)\,r_1 + r_0\right]} + \frac{2r}{m}\sum_{i=2}^{m} \frac{g_{1,1}^{(i)} S_{1,i}^2 - 2g_{1,2}^{(i)} S_{1,i} S_{2,i} + g_{2,2}^{(i)} S_{2,i}^2}{\Delta F_n^{(i)} + (2h_1 - 1)\,\Delta F_{n-1}^{(i)} - 2h_1}. \tag{4.1}$$

When $r_2 = r$, the cobweb network transforms into the conventional cobweb network, as shown in Figure 1(c). The equivalent resistance is

$$R_{m\times n}(d_1, d_2) = \frac{4r}{2m+1}\sum_{i=1}^{m} \frac{g_{1,1}^{(i)} S_{1,i}^2 - 2g_{1,2}^{(i)} S_{1,i} S_{2,i} + g_{2,2}^{(i)} S_{2,i}^2}{\Delta F_n^{(i)} + (2h_1 - 1)\,\Delta F_{n-1}^{(i)} - 2h_1}. \tag{4.2}$$

When $r_2 = 2r$, we have

$$R_{m\times n}(d_1, d_2) = \frac{2r}{m}\sum_{i=1}^{m} \frac{g_{1,1}^{(i)} S_{1,i}^2 - 2g_{1,2}^{(i)} S_{1,i} S_{2,i} + g_{2,2}^{(i)} S_{2,i}^2}{\Delta F_n^{(i)} + (2h_1 - 1)\,\Delta F_{n-1}^{(i)} - 2h_1}. \tag{4.3}$$

The relevant parameters are as follows:

$$g_{k,s}^{(i)} = (t_i - 2)\,(1 - h_1)\,F_{x_k}^{(i)} F_{n-x_s}^{(i)} + h_1 (F_{n-|x_k - x_s|}^{(i)} + F_{|x_k - x_s|}^{(i)}), \tag{4.4}$$

$$F_k^{(i)} = \frac{(\lambda_i^k - \bar{\lambda}_i^k)}{(\lambda_i - \bar{\lambda}_i)},\ \ \Delta F_k^{(i)} = F_{k+1}^{(i)} - F_k^{(i)}, \tag{4.5}$$

$$h = r/r_0,\ \ h_k = r_k/r_0,\ \ S_{k,i} = \sin(y_k \theta_i)\ \ (k = 1, 2),\ t_i = \lambda_i + \bar{\lambda}_i = 2\,(1 + h - h\cos\theta_i)\,, \tag{4.6}$$

where $\lambda_i \overline{\lambda_i} = 1$, $\theta_i = \left\{\frac{(i-1)\pi}{m},\ \frac{(2i-1)\pi}{2m+1},\ \frac{(2i-1)\pi}{2m}\right\}$, and λ_i, $\bar{\lambda}_i$ are expressed as

$$\lambda_i = 1 + h - h\cos\theta_i + \sqrt{(1 + h - h\cos\theta_i)^2 - 1},$$

$$\overline{\lambda_i} = 1 + h - h\cos\theta_i - \sqrt{(1 + h - h\cos\theta_i)^2 - 1}.$$

5. New formulas optimized by Chebyshev polynomials

This section presents the re-expressed Eqs (4.1)–(4.3) of the resistor network. The formulas expressed by the Chebyshev polynomial of the second class can improve the running speed of computers in related aspects.

The accurate equivalent resistance formulas of any two nodes $d(x, y)$ in the $m \times n$ cobweb resistor network are as follows.
When $r_2 = 0$,

$$R_{m\times n}(d_1, d_2) = \frac{r_0 r_1 (y_2 - y_1)^2}{m\left[(n-1)\, r_1 + r_0\right]} + \frac{2r}{m} \sum_{i=2}^{m} \frac{l_{1,1}^{(i)} S_{1,i}^2 - 2l_{1,2}^{(i)} S_{1,i} S_{2,i} + l_{2,2}^{(i)} S_{2,i}^2}{\Delta U_{n-1}^{(i)} + (2h_1 - 1)\, \Delta U_{n-2}^{(i)} - 2h_1}, \tag{5.1}$$

where $S_{k,i} = \sin(y_k \theta_i)\, (k = 1,\ 2)$ and $\theta_i = \frac{(i-1)\pi}{m}$.
When $r_2 = r$,

$$R_{m\times n}(d_1, d_2) = \frac{4r}{2m+1} \sum_{i=1}^{m} \frac{l_{1,1}^{(i)} S_{1,i}^2 - 2l_{1,2}^{(i)} S_{1,i} S_{2,i} + l_{2,2}^{(i)} S_{2,i}^2}{\Delta U_{n-1}^{(i)} + (2h_1 - 1)\, \Delta U_{n-2}^{(i)} - 2h_1}, \tag{5.2}$$

where $S_{k,i} = \sin(y_k \theta_i)\, (k = 1,\ 2)$ and $\theta_i = \frac{(2i-1)\pi}{2m+1}$.
When $r_2 = 2r$,

$$R_{m\times n}(d_1, d_2) = \frac{2r}{m} \sum_{i=1}^{m} \frac{l_{1,1}^{(i)} S_{1,i}^2 - 2l_{1,2}^{(i)} S_{1,i} S_{2,i} + l_{2,2}^{(i)} S_{2,i}^2}{\Delta U_{n-1}^{(i)} + (2h_1 - 1)\, \Delta U_{n-2}^{(i)} - 2h_1}, \tag{5.3}$$

where $S_{k,i} = \sin(y_k \theta_i)\, (k = 1,\ 2)$ and $\theta_i = \frac{(2i-1)\pi}{2m}$.
The relevant parameters are as follows:

$$l_{k,s}^{(i)} = (t_i - 2)\,(1 - h_1)\, U_{x_k-1}^{(i)} U_{n-x_s-1}^{(i)} + h_1 (U_{n-|x_k-x_s|-1}^{(i)} + U_{|x_k-x_s|-1}^{(i)}), \tag{5.4}$$

$$\Delta U_k^{(i)} = U_{k+1}^{(i)} - U_k^{(i)}, \tag{5.5}$$

$$h = r/r_0,\ \ h_k = r_k/r_0, \tag{5.6}$$

$$U_\tau^{(i)} = U_\tau^{(i)}(\cosh\psi_i) = \frac{\sinh(\tau+1)\psi_i}{\sinh(\psi_i)},\ \cosh\psi_i = \frac{t_i}{2},\ \ \frac{t_i}{2} > 1,\ \ \psi_i > 0, \tag{5.7}$$

$$t_i = 2 + \frac{2r}{r_0} - \frac{2r}{r_0}\cos\theta_i, \tag{5.8}$$

where

$$\tau = n-1,\ n-2,\ x_k - 1,\ n - x_s - 1,\ n + x_k - x_s - 1,\ x_s - x_k - 1$$
$$k = 1,\ 2,\ s = 1,\ 2,\ i = 1,\ 2, \ldots,\ m,\ \theta_i = \tfrac{(i-1)\pi}{m},\ \tfrac{(2i-1)\pi}{2m+1},\ \tfrac{(2i-1)\pi}{2m}.$$

To calculate the equivalent resistance $R_{m\times n}(d_1, d_2)$, we introduce a current (J) between points $d_1(x_1, y_1)$ and $d_2(x_2, y_2)$. Using Ohm's law, we can measure the potential difference along a path from $d_1(x_1, y_1)$ to O and then to $d_2(x_2, y_2)$, so we can obtain

$$R_{m\times n}(d_1, d_2) = \frac{V_{Od_2} - V_{Od_1}}{J} = \frac{r_0}{J}\Big(\sum_{i=1}^{y_2} I_{x_2}^{(i)} - \sum_{i=1}^{y_1} I_{x_1}^{(i)}\Big). \tag{5.9}$$

6. Method and derivation of the new formulas

In this section, in order to improve the actual performance, we introduce Horadam sequence [71] represented by the Chebyshev polynomial of the second class [72]. By applying the represented Hadamard sequence to the optimization process of the original equivalent resistance formulas, the purpose of improving computational efficiency is achieved.

6.1. Method

Chebyshev polynomial of the second class has excellent mathematical properties, which can transform complex Hadamard sequences into a series of simple polynomial calculations, thereby improving the efficiency of large-scale data computation. In this paper, the derivation of the optimized equivalent resistance formulas is based on the Chebyshev polynomial of the second class.

The Horadam sequence is defined by the following conditions:

$$W_\tau = dW_{\tau-1} - qW_{\tau-2}, \quad W_0 = A, \quad W_1 = B, \tag{6.1}$$

where $\tau \in \mathbf{N}$, $\tau \geq 2$, $A,\ B,\ d,\ q \in \mathbf{C}$, $\mathbf{N}$ is the set of all natural numbers and $\mathbf{C}$ is the set of all complex numbers.

We know that the Horadam sequence represented by the Chebyshev polynomial of the second class is

$$W_\tau = (\sqrt{q})^\tau \left(\frac{B}{\sqrt{q}} U_{\tau-1}\left(\frac{d}{2\sqrt{q}}\right) - AU_{\tau-2}\left(\frac{d}{2\sqrt{q}}\right)\right), \tag{6.2}$$

where

$$U_\tau = U_\tau(\cos\varphi) = \frac{\sin(\tau+1)\varphi}{\sin\varphi}, \quad \cos\varphi = \frac{d}{2\sqrt{q}},\ \varphi \in \mathbf{C}. \tag{6.3}$$

6.2. Derivation of the new formulas

To start, considering the actual physical context of the resistor network, the Chebyshev polynomial of the second class needs to be re-expressed through hyperbolic functions, then Eq (6.3) is transformed into

$$U_\tau = U_\tau(\cosh\psi) = \frac{\sinh(\tau+1)\psi}{\sinh\psi}, \quad \cosh\psi = \frac{d}{2\sqrt{q}},\ \psi = i\varphi, \tag{6.4}$$

where i is the imaginary unit.

Next, we will present the derivation of Eq (4.5) represented by the Chebyshev polynomial of the second class.

Remark 1: It can be obtained from Eq (4.6) that $t_i = \lambda_i + \bar{\lambda}_i$ and $\lambda_i\overline{\lambda_i} = 1$. Adding these conditions to Eq (6.1), we get the following special Horadam sequence:

$$F_\tau^{(i)} = t_i F_{\tau-1}^{(i)} - F_{\tau-2}^{(i)}, \quad F_0^{(i)} = 0, \quad F_1^{(i)} = 1, \tag{6.5}$$

where $d = t_i > 2$, $q = 1$. By replacing the expression of Eq (4.5) with the results of Eq (6.4), the expression for $F_\tau^{(i)}$ and $\Delta F_\tau^{(i)}$ can be obtained:

$$F_\tau^{(i)} = \frac{\lambda_i^\tau - \bar{\lambda}_i^\tau}{\lambda_i - \bar{\lambda}_i} = U_{\tau-1}^{(i)}(\frac{t_i}{2}), \quad \Delta F_\tau^{(i)} = F_{\tau+1}^{(i)} - F_\tau^{(i)} = U_\tau^{(i)}\left(\frac{t_i}{2}\right) - U_{\tau-1}^{(i)}\left(\frac{t_i}{2}\right). \tag{6.6}$$

Finally, using Eqs (4.1), (6.6), Eqs (4.2), (6.6), and Eqs (4.3), (6.6), the accurate equivalent resistance formulas (5.1)–(5.3) can be individually derived. To clarify the process of transforming the original formulas into the new ones using the Chebyshev polynomials of the second kind, we will provide a detailed explanation below.

Remark 2: In Eq (4.4), $g_{k,s}^{(i)}$ can be reformulated and defined based on Eq (6.6).
When $k = s = 1$,

$$\begin{aligned} g_{1,1}^{(i)} &= (t_i - 2)(1 - h_1) F_{x_1}^{(i)} F_{n-x_1}^{(i)} + h_1(F_n^{(i)} + F_0^{(i)}) \\ &= (t_i - 2)(1 - h_1) U_{x_1-1}^{(i)} U_{n-x_1-1}^{(i)} + h_1(U_{n-1}^{(i)} + U_{-1}^{(i)}) \triangleq l_{1,1}^{(i)}. \end{aligned} \tag{6.7}$$

When $k = 1$ and $s = 2$,

$$\begin{aligned} g_{1,2}^{(i)} &= (t_i - 2)(1 - h_1) F_{x_1}^{(i)} F_{n-x_2}^{(i)} + h_1(F_{n-|x_1-x_2|}^{(i)} + F_{|x_1-x_2|}^{(i)}) \\ &= (t_i - 2)(1 - h_1) U_{x_1-1}^{(i)} U_{n-x_2-1}^{(i)} + h_1(U_{n-|x_1-x_2|-1}^{(i)} + U_{|x_1-x_2|-1}^{(i)}) \triangleq l_{1,2}^{(i)}. \end{aligned} \tag{6.8}$$

When $k = s = 2$,

$$\begin{aligned} g_{2,2}^{(i)} &= (t_i - 2)(1 - h_1) F_{x_2}^{(i)} F_{n-x_2}^{(i)} + h_1(F_n^{(i)} + F_0^{(i)}) \\ &= (t_i - 2)(1 - h_1) U_{x_2-1}^{(i)} U_{n-x_2-1}^{(i)} + h_1(U_{n-1}^{(i)} + U_{-1}^{(i)}) \triangleq l_{2,2}^{(i)}. \end{aligned} \tag{6.9}$$

Similarly, for $\Delta F_k^{(i)}$ in Eq (4.5), when $k = n$ and $k = n-1$, respectively, based on Eq (6.6), the following expressions can be derived:

$$\Delta F_n^{(i)} = F_{n+1}^{(i)} - F_n^{(i)} = U_n^{(i)} - U_{n-1}^{(i)} \triangleq \Delta U_{n-1}^{(i)}, \tag{6.10}$$

$$\Delta F_{n-1}^{(i)} = F_n^{(i)} - F_{n-1}^{(i)} = U_{n-1}^{(i)} - U_{n-2}^{(i)} \triangleq \Delta U_{n-2}^{(i)}, \tag{6.11}$$

By combining Eqs (4.1)–(4.3) with Eqs (6.7)–(6.11), respectively, we obtain Eqs (5.1)–(5.3).

7. Special cases and 3D visualization

Based on equivalent resistance formulas (5.1)–(5.3), this section will examine the impact of varying parameters on the equivalent resistance formulas. Utilizing specific given conditions, we will generate 3D surface plots to visually depict these effects.

When $r_2 = \{0,\ r,\ 2r\}$, and assuming uniform resistance values of $r = r_0 = r_1 = 1$ (*i.e.*, $h = h_1 = 1$), we can derive the formula for the equivalent resistance between specific points $d_1(x_1, y_1)$ and $d_2(x_2, y_2)$.

Case 1. When $r_2 = 0$, $d_1 = (20, 30)$, and $d_2 = (x_2, y_2)$, the equivalent resistance formula is given by:

$$R_{m\times n}(d_1, d_2) = \frac{(y_2 - 30)^2}{mn} + \frac{2}{m}\sum_{i=2}^{m} \frac{l_{1,1}^{(i)} S_{30,i}^2 - 2l_{1,2}^{(i)} S_{30,i} S_{y_2,i} + l_{2,2}^{(i)} S_{y_2,i}^2}{\Delta U_{n-1}^{(i)} + \Delta U_{n-2}^{(i)} - 2}, \tag{7.1}$$

where $S_{y,i} = \sin\frac{y(i-1)\pi}{m}$, $l_{k,s}^{(i)}$ is defined in Eq (5.4), $\Delta U_v^{(i)}$ is defined in Eq (5.5), and $y = 30,\ y_2$, $k = 1,\ 2$, $s = 1,\ 2$, $v = n-1,\ n-2$, $i = 2,\ 3, \ldots,\ m$.

Let $m = n = 75,\ x_1 = 20,\ y_1 = 30$. Then, a special equivalent resistance formula is obtained as follows:

$$R_{75\times 75}(\{20, 30\}, \{x_2, y_2\}) = \frac{(y_2 - 30)^2}{75 \times 75} + \frac{2}{75}\sum_{i=2}^{75} \frac{l_{1,1}^{(i)} S_{30,i}^2 - 2l_{1,2}^{(i)} S_{30,i} S_{y_2,i} + l_{2,2}^{(i)} S_{y_2,i}^2}{\Delta U_{74}^{(i)} + \Delta U_{73}^{(i)} - 2}, \tag{7.2}$$

where $S_{y,i} = \sin\frac{y(i-1)\pi}{75}$, $l_{k,s}^{(i)}$ is defined in Eq (5.4), $\Delta U_v^{(i)}$ is defined in Eq (5.5), and $y = 30,\ y_2$, $k = 1,\ 2$, $s = 1,\ 2$, $v = 74,\ 73$, $i = 2,\ 3, \ldots,\ 75$.

When $r_2 = r$, $d_1 = (20, 30)$, and $d_2 = (x_2, y_2)$, the equivalent resistance formula is given by:

$$R_{m\times n}(d_1, d_2) = \frac{4}{2m+1}\sum_{i=1}^{m}\frac{l_{1,1}^{(i)}S_{30,i}^2 - 2l_{1,2}^{(i)}S_{30,i}S_{y_2,i} + l_{2,2}^{(i)}S_{y_2,i}^2}{\Delta U_{n-1}^{(i)} + \Delta U_{n-2}^{(i)} - 2}, \tag{7.3}$$

where $S_{y,i} = \sin\frac{y(2i-1)\pi}{2m+1}$, $l_{k,s}^{(i)}$ is defined in Eq (5.4), $\Delta U_v^{(i)}$ is defined in Eq (5.5), and $y = 30,\ y_2$, $k = 1,\ 2$, $s = 1,\ 2$, $v = n-1,\ n-2$, $i = 1,\ 2, \ldots,\ m$.

Let $m = n = 75,\ x_1 = 20,\ y_1 = 30$. Then, a special equivalent resistance formula is obtained as follows:

$$R_{75\times 75}(\{20, 30\}, \{x_2, y_2\}) = \frac{4}{151}\sum_{i=1}^{75}\frac{l_{1,1}^{(i)}S_{30,i}^2 - 2l_{1,2}^{(i)}S_{30,i}S_{y_2,i} + l_{2,2}^{(i)}S_{y_2,i}^2}{\Delta U_{74}^{(i)} + \Delta U_{73}^{(i)} - 2}, \tag{7.4}$$

where $S_{y,i} = \sin\frac{y(2i-1)\pi}{151}$, $l_{k,s}^{(i)}$ is defined in Eq (5.4), $\Delta U_v^{(i)}$ is defined in Eq (5.5), and $y = 30,\ y_2$, $k = 1,\ 2$, $s = 1,\ 2$, $v = 74,\ 73$, $i = 1,\ 2, \ldots,\ 75$.

When $r_2 = 2r$, $d_1 = (20, 30)$, and $d_2 = (x_2, y_2)$, the equivalent resistance formula is given by:

$$R_{m\times n}(d_1, d_2) = \frac{2}{m}\sum_{i=1}^{m}\frac{l_{1,1}^{(i)}S_{30,i}^2 - 2l_{1,2}^{(i)}S_{30,i}S_{y_2,i} + l_{2,2}^{(i)}S_{y_2,i}^2}{\Delta U_{n-1}^{(i)} + \Delta U_{n-2}^{(i)} - 2}, \tag{7.5}$$

where $S_{y,i} = \sin\frac{y(2i-1)\pi}{2m}$, $l_{k,s}^{(i)}$ is defined in Eq (5.4), $\Delta U_v^{(i)}$ is defined in Eq (5.5), and $y = 30,\ y_2$, $k = 1,\ 2$, $s = 1,\ 2$, $v = n-1,\ n-2$, $i = 1,\ 2, \ldots,\ m$.

Let $m = n = 75,\ x_1 = 20,\ y_1 = 30$. Then, a special equivalent resistance formula is obtained as follows:

$$R_{75\times 75}(\{20, 30\}, \{x_2, y_2\}) = \frac{2}{75}\sum_{i=1}^{75}\frac{l_{1,1}^{(i)}S_{30,i}^2 - 2l_{1,2}^{(i)}S_{30,i}S_{y_2,i} + l_{2,2}^{(i)}S_{y_2,i}^2}{\Delta U_{74}^{(i)} + \Delta U_{73}^{(i)} - 2}, \tag{7.6}$$

where $S_{y,i} = \sin\frac{y(2i-1)\pi}{150}$, $l_{k,s}^{(i)}$ is defined in Eq (5.4), $\Delta U_v^{(i)}$ is defined in Eq (5.5), and $y = 30,\ y_2$, $k = 1,\ 2$, $s = 1,\ 2$, $v = 74,\ 73$, $i = 1,\ 2, \ldots,\ 75$.

The three-dimensional surface plot of the equivalent resistance between points $d_1\,(20, 30)$ and $d_2(x_2, y_2)$ is shown in Figure 5.

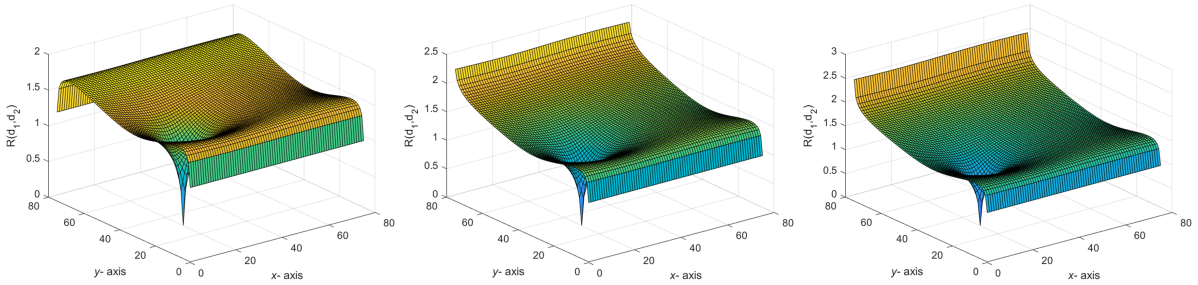

(a) **(b)** **(c)**

Figure 5. **(a)** is the 3D distribution map of equivalent resistance in Eq (7.2); **(b)** is the 3D distribution map of equivalent resistance in Eq (7.4); **(c)** is the 3D distribution map of equivalent resistance in Eq (7.6).

Case 2. When $r_2 = 0$, $d_1 = (20, y_2)$, and $d_2 = (x_2, y_2)$, the equivalent resistance formula is given by:

$$R_{m\times n}(d_1, d_2) = \frac{2}{m}\sum_{i=2}^{m}\frac{l_{1,1}^{(i)}S_{y_2,i}^2 + \left(l_{2,2}^{(i)} - 2l_{1,2}^{(i)}\right)S_{y_2,i}^2}{\Delta U_{n-1}^{(i)} + \Delta U_{n-2}^{(i)} - 2}, \tag{7.7}$$

where $S_{y,i} = \sin\frac{y(i-1)\pi}{m}$, $l_{k,s}^{(i)}$ is defined in Eq (5.4), $\Delta U_v^{(i)}$ is defined in Eq (5.5), and $y = y_2$, $k = 1,\ 2$, $s = 1,\ 2$, $v = n-1,\ n-2$, $i = 2,\ 3, \ldots,\ m$.

Let $m = n = 75,\ x_1 = 20,\ y_1 = y_2$. Then, a special equivalent resistance formula is obtained as follows:

$$R_{75\times 75}(\{20, y_2\}, \{x_2, y_2\}) = \frac{2}{75}\sum_{i=2}^{75}\frac{l_{1,1}^{(i)}S_{y_2,i}^2 + \left(l_{2,2}^{(i)} - 2l_{1,2}^{(i)}\right)S_{y_2,i}^2}{\Delta U_{74}^{(i)} + \Delta U_{73}^{(i)} - 2}, \tag{7.8}$$

where $S_{y,i} = \sin\frac{y(i-1)\pi}{75}$, $l_{k,s}^{(i)}$ is defined in Eq (5.4), $\Delta U_v^{(i)}$ is defined in Eq (5.5), and $y = y_2$, $k = 1,\ 2$, $s = 1,\ 2$, $v = 74,\ 73$, $i = 2,\ 3, \ldots,\ 75$.

When $r_2 = r$, $d_1 = (20, y_2)$, and $d_2 = (x_2, y_2)$, the equivalent resistance formula is given by:

$$R_{m\times n}(d_1, d_2) = \frac{4}{2m+1}\sum_{i=1}^{m}\frac{l_{1,1}^{(i)}S_{y_2,i}^2 + \left(l_{2,2}^{(i)} - 2l_{1,2}^{(i)}\right)S_{y_2,i}^2}{\Delta U_{n-1}^{(i)} + \Delta U_{n-2}^{(i)} - 2}, \tag{7.9}$$

where $S_{y,i} = \sin\frac{y(2i-1)\pi}{2m+1}$, $l_{k,s}^{(i)}$ is defined in Eq (5.4), $\Delta U_v^{(i)}$ is defined in Eq (5.5), and $y = y_2$, $k = 1,\ 2$, $s = 1,\ 2$, $v = n-1,\ n-2$, $i = 1,\ 2, \ldots,\ m$.

Let $m = n = 75,\ x_1 = 20,\ y_1 = y_2$. Then, a special equivalent resistance formula is obtained as follows:

$$R_{75\times 75}(\{20, y_2\}, \{x_2, y_2\}) = \frac{4}{151}\sum_{i=1}^{75}\frac{l_{1,1}^{(i)}S_{y_2,i}^2 + \left(l_{2,2}^{(i)} - 2l_{1,2}^{(i)}\right)S_{y_2,i}^2}{\Delta U_{74}^{(i)} + \Delta U_{73}^{(i)} - 2}, \tag{7.10}$$

where $S_{y,i} = \sin\frac{y(2i-1)\pi}{151}$, $l_{k,s}^{(i)}$ is defined in Eq (5.4), $\Delta U_v^{(i)}$ is defined in Eq (5.5), and $y = y_2$, $k = 1,\ 2$, $s = 1,\ 2$, $v = 74,\ 73$, $i = 1,\ 2, \ldots,\ 75$.

When $r_2 = 2r$, $d_1 = (20, y_2)$, and $d_2 = (x_2, y_2)$, the equivalent resistance formula is given by:

$$R_{m\times n}(d_1, d_2) = \frac{2}{m}\sum_{i=1}^{m}\frac{l_{1,1}^{(i)}S_{y_2,i}^2 + \left(l_{2,2}^{(i)} - 2l_{1,2}^{(i)}\right)S_{y_2,i}^2}{\Delta U_{n-1}^{(i)} + \Delta U_{n-2}^{(i)} - 2}, \tag{7.11}$$

where $S_{y,i} = \sin\frac{y(2i-1)\pi}{2m}$, $l_{k,s}^{(i)}$ is defined in Eq (5.4), $\Delta U_v^{(i)}$ is defined in Eq (5.5), and $y = y_2$, $k = 1,\ 2$, $s = 1,\ 2$, $v = n-1,\ n-2$, $i = 1,\ 2, \ldots,\ m$.

Let $m = n = 75,\ x_1 = 20,\ y_1 = 30$. Then, a special equivalent resistance formula is obtained as follows:

$$R_{75\times75}(\{20, y_2\}, \{x_2, y_2\}) = \frac{2}{75}\sum_{i=1}^{75}\frac{l_{1,1}^{(i)}S_{y_2,i}^2 + \left(l_{2,2}^{(i)} - 2l_{1,2}^{(i)}\right)S_{y_2,i}^2}{\Delta U_{74}^{(i)} + \Delta U_{73}^{(i)} - 2}, \tag{7.12}$$

where $S_{y,i} = \sin\frac{y(2i-1)\pi}{150}$, $l_{k,s}^{(i)}$ is defined in Eq (5.4), $\Delta U_v^{(i)}$ is defined in Eq (5.5), and $y = y_2$, $k = 1,\ 2$, $s = 1,\ 2$, $v = 74,\ 73$, $i = 1,\ 2, \ldots,\ 75$.

The three-dimensional surface plot of the equivalent resistance between points $d_1\,(20, y_2)$ and $d_2(x_2, y_2)$ is shown in Figure 6.

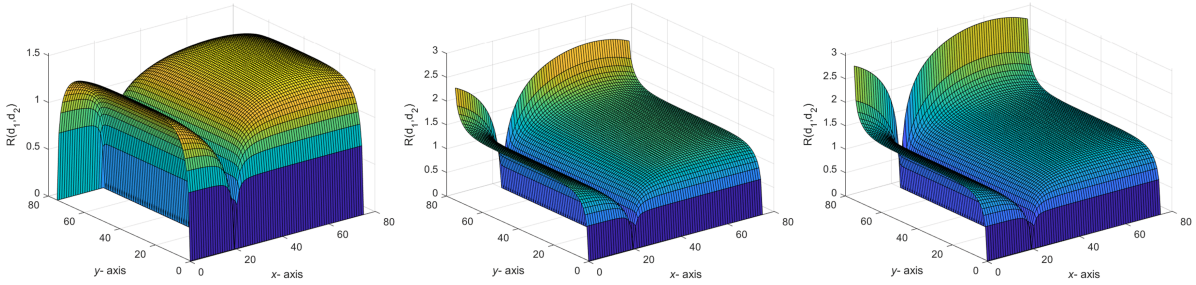

(a) **(b)** **(c)**

Figure 6. **(a)** is the 3D distribution map of equivalent resistance in Eq (7.8); **(b)** is the 3D distribution map of equivalent resistance in Eq (7.10); **(c)** is the 3D distribution map of equivalent resistance in Eq (7.12).

Case 3. When $r_2 = 0$, $d_1 = (20, x_2)$, and $d_2 = (x_2, y_2)$, the equivalent resistance formula is given by:

$$R_{m\times n}(d_1, d_2) = \frac{(y_2 - x_2)^2}{mn} + \frac{2}{m}\sum_{i=2}^{m}\frac{l_{1,1}^{(i)}S_{x_2,i}^2 - 2l_{1,2}^{(i)}S_{x_2,i}S_{y_2,i} + l_{2,2}^{(i)}S_{y_2,i}^2}{\Delta U_{n-1}^{(i)} + \Delta U_{n-2}^{(i)} - 2}, \tag{7.13}$$

where $S_{y,i} = \sin\frac{y(i-1)\pi}{m}$, $l_{k,s}^{(i)}$ is defined in Eq (5.4), $\Delta U_v^{(i)}$ is defined in Eq (5.5), and $y = x_2,\ y_2$, $k = 1,\ 2$, $s = 1,\ 2$, $v = n-1,\ n-2$, $i = 2,\ 3, \ldots,\ m$.

Let $m = n = 75,\ x_1 = 20,\ y_1 = x_2$. Then, a special equivalent resistance formula is obtained as follows:

$$R_{75\times75}(\{20, x_2\}, \{x_2, y_2\}) = \frac{(y_2 - x_2)^2}{75\times75} + \frac{2}{75}\sum_{i=2}^{75}\frac{l_{1,1}^{(i)}S_{x_2,i}^2 - 2l_{1,2}^{(i)}S_{x_2,i}S_{y_2,i} + l_{2,2}^{(i)}S_{y_2,i}^2}{\Delta U_{74}^{(i)} + \Delta U_{73}^{(i)} - 2}, \tag{7.14}$$

where $S_{y,i} = \sin\frac{y(i-1)\pi}{75}$, $l_{k,s}^{(i)}$ is defined in Eq (5.4), $\Delta U_v^{(i)}$ is defined in Eq (5.5), and $y = x_2,\ y_2$, $k = 1,\ 2$, $s = 1,\ 2$, $v = 74,\ 73$, $i = 2,\ 3, \ldots,\ 75$.

When $r_2 = r$, $d_1 = (20, x_2)$, and $d_2 = (x_2, y_2)$, the equivalent resistance formula is given by:

$$R_{m\times n}(d_1, d_2) = \frac{4}{2m+1}\sum_{i=1}^{m}\frac{l_{1,1}^{(i)}S_{x_2,i}^2 - 2l_{1,2}^{(i)}S_{x_2,i}S_{y_2,i} + l_{2,2}^{(i)}S_{y_2,i}^2}{\Delta U_{n-1}^{(i)} + \Delta U_{n-2}^{(i)} - 2}, \tag{7.15}$$

where $S_{y,i} = \sin\frac{y(2i-1)\pi}{2m+1}$, $l_{k,s}^{(i)}$ is defined in Eq (5.4), $\Delta U_v^{(i)}$ is defined in Eq (5.5), and $y = x_2,\ y_2$, $k = 1,\ 2$, $s = 1,\ 2$, $v = n-1,\ n-2$, $i = 1,\ 2, \ldots,\ m$.

Let $m = n = 75,\ x_1 = 20,\ y_1 = x_2$. Then, a special equivalent resistance formula is obtained as follows:

$$R_{75\times75}(\{20, x_2\}, \{x_2, y_2\}) = \frac{4}{151}\sum_{i=1}^{75}\frac{l_{1,1}^{(i)}S_{x_2,i}^2 - 2l_{1,2}^{(i)}S_{x_2,i}S_{y_2,i} + l_{2,2}^{(i)}S_{y_2,i}^2}{\Delta U_{74}^{(i)} + \Delta U_{73}^{(i)} - 2}, \tag{7.16}$$

where $S_{y,i} = \sin\frac{y(2i-1)\pi}{151}$, $l_{k,s}^{(i)}$ is defined in Eq (5.4), $\Delta U_v^{(i)}$ is defined in Eq (5.5), and $y = x_2,\ y_2$, $k = 1,\ 2$, $s = 1,\ 2$, $v = 74,\ 73$, $i = 1,\ 2, \ldots,\ 75$.

When $r_2 = 2r$, $d_1 = (20, x_2)$, and $d_2 = (x_2, y_2)$, the equivalent resistance formula is given by:

$$R_{m\times n}(d_1, d_2) = \frac{2}{m}\sum_{i=1}^{m}\frac{l_{1,1}^{(i)}S_{x_2,i}^2 - 2l_{1,2}^{(i)}S_{x_2,i}S_{y_2,i} + l_{2,2}^{(i)}S_{y_2,i}^2}{\Delta U_{n-1}^{(i)} + \Delta U_{n-2}^{(i)} - 2}, \tag{7.17}$$

where $S_{y,i} = \sin\frac{y(2i-1)\pi}{2m}$, $l_{k,s}^{(i)}$ is defined in Eq (5.4), $\Delta U_v^{(i)}$ is defined in Eq (5.5), and $y = x_2,\ y_2$, $k = 1,\ 2$, $s = 1,\ 2$, $v = n-1,\ n-2$, $i = 1,\ 2, \ldots,\ m$.

Let $m = n = 75,\ x_1 = 20,\ y_1 = 30$. Then, a special equivalent resistance formula is obtained as follows:

$$R_{75\times75}(\{20, x_2\}, \{x_2, y_2\}) = \frac{2}{75}\sum_{i=1}^{75}\frac{l_{1,1}^{(i)}S_{x_2,i}^2 - 2l_{1,2}^{(i)}S_{x_2,i}S_{y_2,i} + l_{2,2}^{(i)}S_{y_2,i}^2}{\Delta U_{74}^{(i)} + \Delta U_{73}^{(i)} - 2}, \tag{7.18}$$

where $S_{y,i} = \sin\frac{y(2i-1)\pi}{150}$, $l_{k,s}^{(i)}$ is defined in Eq (5.4), $\Delta U_v^{(i)}$ is defined in Eq (5.5), and $y = x_2,\ y_2$, $k = 1,\ 2$, $s = 1,\ 2$, $v = 74,\ 73$, $i = 1,\ 2, \ldots,\ 75$.

The three-dimensional surface plot of the equivalent resistance between points $d_1\,(20, x_2)$ and $d_2(x_2, y_2)$ is shown in Figure 7.

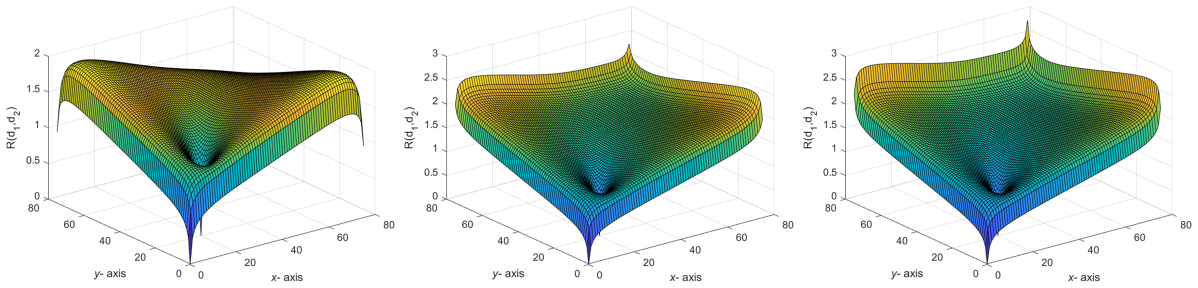

(a) **(b)** **(c)**

Figure 7. **(a)** is the 3D distribution map of equivalent resistance in Eq (7.14); **(b)** is the 3D distribution map of equivalent resistance in Eq (7.16); **(c)** is the 3D distribution map of equivalent resistance in Eq (7.18).

Case 4. When $r_2 = 0$, $d_1 = (x_1, 50)$, and $d_2 = (x_2, 70)$, the equivalent resistance formula is given by:

$$R_{m\times n}(d_1, d_2) = \frac{400}{mn} + \frac{2}{m}\sum_{i=2}^{m}\frac{l_{1,1}^{(i)}S_{50,i}^2 - 2l_{1,2}^{(i)}S_{50,i}S_{70,i} + l_{2,2}^{(i)}S_{70,i}^2}{\Delta U_{n-1}^{(i)} + \Delta U_{n-2}^{(i)} - 2}, \tag{7.19}$$

where $S_{y,i} = \sin\frac{y(i-1)\pi}{m}$, $l_{k,s}^{(i)}$ is defined in Eq (5.4), $\Delta U_v^{(i)}$ is defined in Eq (5.5), and $y = 50,\ 70$, $k = 1,\ 2$, $s = 1,\ 2$, $v = n-1,\ n-2$, $i = 2,\ 3, \ldots,\ m$.

Let $m = 90,\ n = 100,\ y_1 = 50,\ y_2 = 70$. Then, a special equivalent resistance formula is obtained as follows:

$$R_{90\times100}(\{x_1, 50\}, \{x_2, 70\}) = \frac{400}{90\times100} + \frac{1}{45}\sum_{i=2}^{90}\frac{l_{1,1}^{(i)}S_{50,i}^2 - 2l_{1,2}^{(i)}S_{50,i}S_{70,i} + l_{2,2}^{(i)}S_{70,i}^2}{\Delta U_{99}^{(i)} + \Delta U_{98}^{(i)} - 2}, \tag{7.20}$$

where $S_{y,i} = \sin\frac{y(i-1)\pi}{90}$, $l_{k,s}^{(i)}$ is defined in Eq (5.4), $\Delta U_v^{(i)}$ is defined in Eq (5.5), and $y = 50,\ 70$, $k = 1,\ 2$, $s = 1,\ 2$, $v = 99,\ 98$, $i = 2,\ 3, \ldots,\ 90$.

When $r_2 = r$, $d_1 = (x_1, 50)$, and $d_2 = (x_2, 70)$, the equivalent resistance formula is given by:

$$R_{m\times n}(d_1, d_2) = \frac{4}{2m+1}\sum_{i=1}^{m}\frac{l_{1,1}^{(i)}S_{50,i}^2 - 2l_{1,2}^{(i)}S_{50,i}S_{70,i} + l_{2,2}^{(i)}S_{70,i}^2}{\Delta U_{n-1}^{(i)} + \Delta U_{n-2}^{(i)} - 2}, \tag{7.21}$$

where $S_{y,i} = \sin\frac{y(2i-1)\pi}{2m+1}$, $l_{k,s}^{(i)}$ is defined in Eq (5.4), $\Delta U_v^{(i)}$ is defined in Eq (5.5), and $y = 50,\ 70$, $k = 1,\ 2$, $s = 1,\ 2$, $v = n-1,\ n-2$, $i = 1,\ 2, \ldots,\ m$.

Let $m = 90,\ n = 100,\ y_1 = 50,\ y_2 = 70$. Then, a special equivalent resistance formula is obtained as follows:

$$R_{90\times100}(\{x_1, 50\}, \{x_2, 70\}) = \frac{4}{181}\sum_{i=1}^{90}\frac{l_{1,1}^{(i)}S_{50,i}^2 - 2l_{1,2}^{(i)}S_{50,i}S_{70,i} + l_{2,2}^{(i)}S_{70,i}^2}{\Delta U_{99}^{(i)} + \Delta U_{98}^{(i)} - 2}, \tag{7.22}$$

where $S_{y,i} = \sin\frac{y(2i-1)\pi}{181}$, $l_{k,s}^{(i)}$ is defined in Eq (5.4), $\Delta U_v^{(i)}$ is defined in Eq (5.5), and $y = 50,\ 70$, $k = 1,\ 2$, $s = 1,\ 2$, $v = 99,\ 98$, $i = 1,\ 2, \ldots,\ 90$.

When $r_2 = 2r$, $d_1 = (x_1, 50)$, and $d_2 = (x_2, 70)$, the equivalent resistance formula is given by:

$$R_{m\times n}(d_1, d_2) = \frac{2}{m}\sum_{i=1}^{m}\frac{l_{1,1}^{(i)}S_{50,i}^2 - 2l_{1,2}^{(i)}S_{50,i}S_{70,i} + l_{2,2}^{(i)}S_{70,i}^2}{\Delta U_{n-1}^{(i)} + \Delta U_{n-2}^{(i)} - 2}, \tag{7.23}$$

where $S_{y,i} = \sin\frac{y(2i-1)\pi}{2m}$, $l_{k,s}^{(i)}$ is defined in Eq (5.4), $\Delta U_v^{(i)}$ is defined in Eq (5.5), and $y = 50,\ 70$, $k = 1,\ 2$, $s = 1,\ 2$, $v = n-1,\ n-2$, $i = 1,\ 2, \ldots,\ m$.

Let $m = 90,\ n = 100,\ y_1 = 50,\ y_2 = 70$. Then, a special equivalent resistance formula is obtained as follows:

$$R_{90\times100}(\{x_1, 50\}, \{x_2, 70\}) = \frac{1}{45}\sum_{i=1}^{90}\frac{l_{1,1}^{(i)}S_{50,i}^2 - 2l_{1,2}^{(i)}S_{50,i}S_{70,i} + l_{2,2}^{(i)}S_{70,i}^2}{\Delta U_{99}^{(i)} + \Delta U_{98}^{(i)} - 2}, \tag{7.24}$$

where $S_{y,i} = \sin\frac{y(2i-1)\pi}{180}$, $l_{k,s}^{(i)}$ is defined in Eq (5.4), $\Delta U_v^{(i)}$ is defined in Eq (5.5), and $y = 50,\ 70$, $k = 1,\ 2$, $s = 1,\ 2$, $v = 99,\ 98$, $i = 1,\ 2, \ldots,\ 90$.

The three-dimensional surface plot of the equivalent resistance between points $d_1\,(x_1, 50)$ and $d_2(x_2, 70)$ is shown in Figure 8.

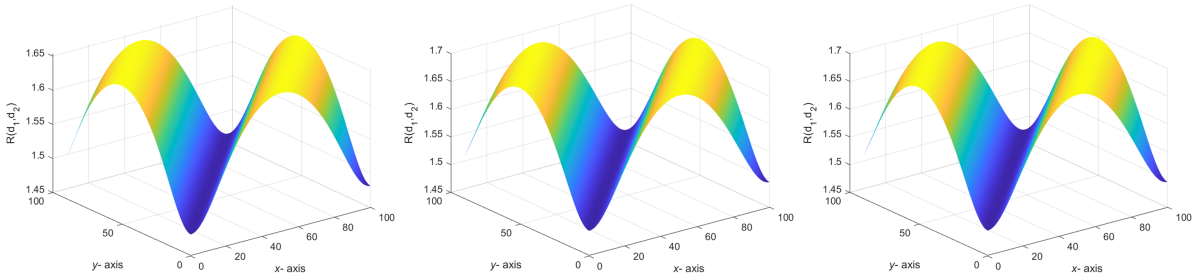

(a) **(b)** **(c)**

Figure 8. **(a)** is the 3D distribution map of equivalent resistance in Eq (7.20); **(b)** is the 3D distribution map of equivalent resistance in Eq (7.22); **(c)** is the 3D distribution map of equivalent resistance in Eq (7.24).

Case 5. When $r_2 = 0$, $d_1 = (y_2, y_2)$, and $d_2 = (x_2, y_2)$, the equivalent resistance formula is given by:

$$R_{m\times n}(d_1, d_2) = \frac{2}{m}\sum_{i=2}^{m}\frac{\left(l_{1,1}^{(i)} - 2l_{1,2}^{(i)} + l_{2,2}^{(i)}\right)S_{y_2,i}^2}{\Delta U_{n-1}^{(i)} + \Delta U_{n-2}^{(i)} - 2}, \tag{7.25}$$

where $S_{y,i} = \sin\frac{y(i-1)\pi}{m}$, $l_{k,s}^{(i)}$ is defined in Eq (5.4), $\Delta U_v^{(i)}$ is defined in Eq (5.5), and $y = y_2$, $k = 1,\ 2$, $s = 1,\ 2$, $v = n-1,\ n-2$, $i = 2,\ 3, \ldots,\ m$.

Let $m = 90,\ n = 100,\ x_1 = y_1 = y_2$. Then, a special equivalent resistance formula is obtained as follows:

$$R_{90\times 100}(\{y_2, y_2\}, \{x_2, y_2\}) = \frac{400}{90\times 100} + \frac{1}{45}\sum_{i=2}^{90}\frac{\left(l_{1,1}^{(i)} - 2l_{1,2}^{(i)} + l_{2,2}^{(i)}\right)S_{y_2,i}^2}{\Delta U_{99}^{(i)} + \Delta U_{98}^{(i)} - 2}, \tag{7.26}$$

where $S_{y,i} = \sin\frac{y(i-1)\pi}{90}$, $l_{k,s}^{(i)}$ is defined in Eq (5.4), $\Delta U_v^{(i)}$ is defined in Eq (5.5), and $y = y_2$, $k = 1,\ 2$, $s = 1,\ 2$, $v = 99,\ 98$, $i = 2,\ 3, \ldots,\ 90$.

When $r_2 = r$, $d_1 = (y_2, y_2)$, and $d_2 = (x_2, y_2)$, the equivalent resistance formula is given by:

$$R_{m\times n}(d_1, d_2) = \frac{4}{2m+1}\sum_{i=1}^{m}\frac{\left(l_{1,1}^{(i)} - 2l_{1,2}^{(i)} + l_{2,2}^{(i)}\right)S_{y_2,i}^2}{\Delta U_{n-1}^{(i)} + \Delta U_{n-2}^{(i)} - 2}, \tag{7.27}$$

where $S_{y,i} = \sin\frac{y(2i-1)\pi}{2m+1}$, $l_{k,s}^{(i)}$ is defined in Eq (5.4), $\Delta U_v^{(i)}$ is defined in Eq (5.5), and $y = y_2$, $k = 1,\ 2$, $s = 1,\ 2$, $v = n-1,\ n-2$, $i = 1,\ 2, \ldots,\ m$.

Let $m = 90,\ n = 100,\ x_1 = y_1 = y_2$. Then, a special equivalent resistance formula is obtained as follows:

$$R_{90\times 100}(\{y_2, y_2\}, \{x_2, y_2\}) = \frac{4}{181}\sum_{i=1}^{90}\frac{\left(l_{1,1}^{(i)} - 2l_{1,2}^{(i)} + l_{2,2}^{(i)}\right)S_{y_2,i}^2}{\Delta U_{99}^{(i)} + \Delta U_{98}^{(i)} - 2}, \tag{7.28}$$

where $S_{y,i} = \sin\frac{y(2i-1)\pi}{181}$, $l_{k,s}^{(i)}$ is defined in Eq (5.4), $\Delta U_v^{(i)}$ is defined in Eq (5.5), and $y = y_2$, $k = 1,\ 2$, $s = 1,\ 2$, $v = 99,\ 98$, $i = 1,\ 2, \ldots,\ 90$.

When $r_2 = 2r$, $d_1 = (y_2, y_2)$, and $d_2 = (x_2, y_2)$, the equivalent resistance formula is given by:

$$R_{m\times n}(d_1, d_2) = \frac{2}{m}\sum_{i=1}^{m}\frac{\left(l_{1,1}^{(i)} - 2l_{1,2}^{(i)} + l_{2,2}^{(i)}\right)S_{y_2,i}^2}{\Delta U_{n-1}^{(i)} + \Delta U_{n-2}^{(i)} - 2}, \tag{7.29}$$

where $S_{y,i} = \sin\frac{y(2i-1)\pi}{2m}$, $l_{k,s}^{(i)}$ is defined in Eq (5.4), $\Delta U_v^{(i)}$ is defined in Eq (5.5), and $y = y_2$, $k = 1,\ 2$, $s = 1,\ 2$, $v = n-1,\ n-2$, $i = 1,\ 2, \ldots,\ m$.

Let $m = 90,\ n = 100,\ x_1 = y_1 = y_2$. Then, a special equivalent resistance formula is obtained as follows:

$$R_{90\times100}(\{y_2, y_2\}, \{x_2, y_2\}) = \frac{1}{45}\sum_{i=1}^{90}\frac{\left(l_{1,1}^{(i)} - 2l_{1,2}^{(i)} + l_{2,2}^{(i)}\right)S_{y_2,i}^2}{\Delta U_{99}^{(i)} + \Delta U_{98}^{(i)} - 2}, \tag{7.30}$$

where $S_{y,i} = \sin\frac{y(2i-1)\pi}{180}$, $l_{k,s}^{(i)}$ is defined in Eq (5.4), $\Delta U_v^{(i)}$ is defined in Eq (5.5), and $y = y_2$, $k = 1,\ 2$, $s = 1,\ 2$, $v = 99,\ 98$, $i = 1,\ 2, \ldots,\ 90$.

The three-dimensional surface plot of the equivalent resistance between points $d_1(y_2, y_2)$ and $d_2(x_2, y_2)$ is shown in Figure 9.

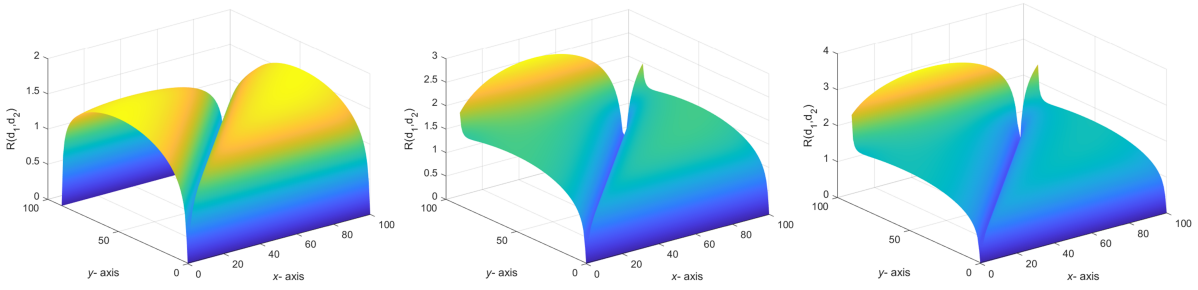

(a) **(b)** **(c)**

Figure 9. **(a)** is the 3D distribution map of equivalent resistance in Eq (7.26); **(b)** is the 3D distribution map of equivalent resistance in Eq (7.28); **(c)** is the 3D distribution map of equivalent resistance in Eq (7.30).

Case 6. When $r_2 = 0$, $d_1 = (y_2, x_2)$, and $d_2 = (x_2, y_2)$, the equivalent resistance formula is given by:

$$R_{m\times n}(d_1, d_2) = \frac{(y_2 - x_2)^2}{mn} + \frac{2}{m}\sum_{i=2}^{m}\frac{l_{1,1}^{(i)}S_{x_2,i}^2 - 2l_{1,2}^{(i)}S_{x_2,j}S_{y_2,i} + l_{2,2}^{(i)}S_{y_2,i}^2}{\Delta U_{n-1}^{(i)} + \Delta U_{n-2}^{(i)} - 2}, \tag{7.31}$$

where $S_{y,i} = \sin\frac{y(i-1)\pi}{m}$, $l_{k,s}^{(i)}$ is defined in Eq (5.4), $\Delta U_v^{(i)}$ is defined in Eq (5.5), and $y = x_2,\ y_2$, $k = 1,\ 2$, $s = 1,\ 2$, $v = n-1,\ n-2$, $i = 2,\ 3, \ldots,\ m$.

Let $m = 90,\ n = 100,\ x_1 = y_2,\ y_1 = x_2$. Then, a special equivalent resistance formula is obtained as follows:

$$R_{90\times100}(\{y_2, x_2\}, \{x_2, y_2\}) = \frac{(y_2 - x_2)^2}{90\times100} + \frac{1}{45}\sum_{i=2}^{90}\frac{l_{1,1}^{(i)}S_{x_2,i}^2 - 2l_{1,2}^{(i)}S_{x_2,j}S_{y_2,i} + l_{2,2}^{(i)}S_{y_2,i}^2}{\Delta U_{99}^{(i)} + \Delta U_{98}^{(i)} - 2}, \tag{7.32}$$

where $S_{y,i} = \sin\frac{y(i-1)\pi}{90}$, $l_{k,s}^{(i)}$ is defined in Eq (5.4), $\Delta U_v^{(i)}$ is defined in Eq (5.5), and $y = x_2,\ y_2$, $k = 1,\ 2$, $s = 1,\ 2$, $v = 99,\ 98$, $i = 2,\ 3, \ldots,\ 90$.

When $r_2 = r$, $d_1 = (y_2, x_2)$, and $d_2 = (x_2, y_2)$, the equivalent resistance formula is given by:

$$R_{m\times n}(d_1, d_2) = \frac{4}{2m+1}\sum_{i=1}^{m}\frac{l_{1,1}^{(i)}S_{x_2,i}^2 - 2l_{1,2}^{(i)}S_{x_2,j}S_{y_2,i} + l_{2,2}^{(i)}S_{y_2,i}^2}{\Delta U_{n-1}^{(i)} + \Delta U_{n-2}^{(i)} - 2}, \tag{7.33}$$

where $S_{y,i} = \sin\frac{y(2i-1)\pi}{2m+1}$, $l_{k,s}^{(i)}$ is defined in Eq (5.4), $\Delta U_v^{(i)}$ is defined in Eq (5.5), and $y = x_2,\ y_2$, $k = 1,\ 2$, $s = 1,\ 2$, $v = n-1,\ n-2$, $i = 1,\ 2, \ldots,\ m$.

Let $m = 90,\ n = 100,\ x_1 = y_2,\ y_1 = x_2$. Then, a special equivalent resistance formula is obtained as follows:

$$R_{90\times100}(\{y_2, x_2\}, \{x_2, y_2\}) = \frac{4}{181}\sum_{i=1}^{90}\frac{l_{1,1}^{(i)}S_{x_2,i}^2 - 2l_{1,2}^{(i)}S_{x_2,j}S_{y_2,i} + l_{2,2}^{(i)}S_{y_2,i}^2}{\Delta U_{99}^{(i)} + \Delta U_{98}^{(i)} - 2}, \tag{7.34}$$

where $S_{y,i} = \sin\frac{y(2i-1)\pi}{181}$, $l_{k,s}^{(i)}$ is defined in Eq (5.4), $\Delta U_v^{(i)}$ is defined in Eq (5.5), and $y = x_2,\ y_2$, $k = 1,\ 2$, $s = 1,\ 2$, $v = 99,\ 98$, $i = 1,\ 2, \ldots,\ 90$.

When $r_2 = 2r$, $d_1 = (y_2, x_2)$, and $d_2 = (x_2, y_2)$, the equivalent resistance formula is given by:

$$R_{m\times n}(d_1, d_2) = \frac{2}{m}\sum_{i=1}^{m}\frac{l_{1,1}^{(i)}S_{x_2,i}^2 - 2l_{1,2}^{(i)}S_{x_2,j}S_{y_2,i} + l_{2,2}^{(i)}S_{y_2,i}^2}{\Delta U_{n-1}^{(i)} + \Delta U_{n-2}^{(i)} - 2}, \tag{7.35}$$

where $S_{y,i} = \sin\frac{y(2i-1)\pi}{2m}$, $l_{k,s}^{(i)}$ is defined in Eq (5.4), $\Delta U_v^{(i)}$ is defined in Eq (5.5), and $y = x_2,\ y_2$, $k = 1,\ 2$, $s = 1,\ 2$, $v = n-1,\ n-2$, $i = 1,\ 2, \ldots,\ m$.

Let $m = 90,\ n = 100,\ x_1 = y_2,\ y_1 = x_2$. Then, a special equivalent resistance formula is obtained as follows:

$$R_{90\times100}(\{y_2, x_2\}, \{x_2, y_2\}) = \frac{1}{45}\sum_{i=1}^{90}\frac{l_{1,1}^{(i)}S_{x_2,i}^2 - 2l_{1,2}^{(i)}S_{x_2,j}S_{y_2,i} + l_{2,2}^{(i)}S_{y_2,i}^2}{\Delta U_{99}^{(i)} + \Delta U_{98}^{(i)} - 2}, \tag{7.36}$$

where $S_{y,i} = \sin\frac{y(2i-1)\pi}{180}$, $l_{k,s}^{(i)}$ is defined in Eq (5.4), $\Delta U_v^{(i)}$ is defined in Eq (5.5), and $y = x_2,\ y_2$, $k = 1,\ 2$, $s = 1,\ 2$, $v = 99,\ 98$, $i = 1,\ 2, \ldots,\ 90$.

The three-dimensional surface plot of the equivalent resistance between points $d_1\,(y_2, x_2)$ and $d_2(x_2, y_2)$ is shown in Figure 10.

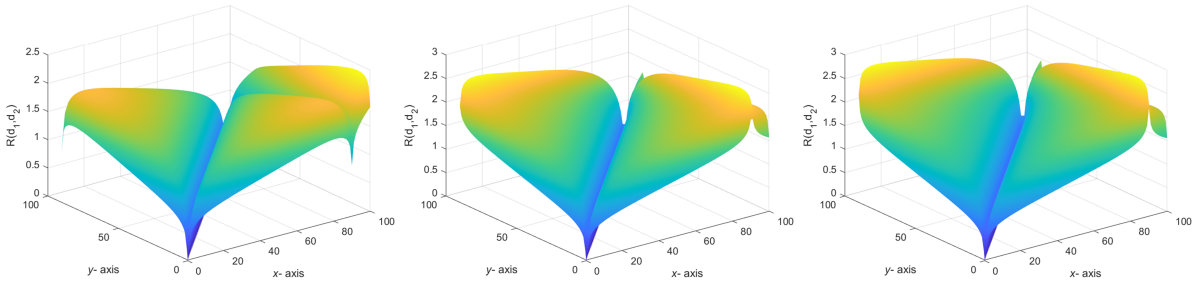

(a) **(b)** **(c)**

Figure 10. **(a)** is the 3D distribution map of equivalent resistance in Eq (7.32); **(b)** is the 3D distribution map of equivalent resistance in Eq (7.34); **(c)** is the 3D distribution map of equivalent resistance in Eq (7.36).

8. Comparison of calculation efficiency

In this section, we will conduct a comparative experiment on the computational efficiency of Eqs (4.1), (5.1), Eqs (4.2), (5.2) and Eqs (4.3), (5.3) under the same scale of resistor network. The calculation scale in this experiment is denoted by $m \times n$, "time" is the time in seconds, and t denotes the

Central Processing Unit (CPU) time taken to calculate the equivalent resistance between points d_2 and d_1. In the experimental results, "−" indicates that the calculation scale beyond the memory limit of Matlab or time exceeds 1200 seconds.

The experiment is completed under the environmental conditions of CPU model Intel Core i5-7300HQ, CPU frequency 2.50 GHz, and Matlab version is R2023b. To simplify the experiment, we define d_1 as the fixed point on the resistor network and d_2 as any point on the resistor network except for the origin d_1. t_1 and t_2 denote total CPU times from all points (excluding point d_1) to d_1 computed by Eqs (4.1)–(4.3) and Eqs (5.1)–(5.3), respectively.

Table 1. The comparison of calculation efficiency for equivalent resistance formulas (4.1) and (5.1).

$m \times n$	r	r_0	r_1	t_1	t_2
100×80	1	1	1	2.1159	0.3200
200×100	1	1	1	10.9268	1.5819
300×200	1	1	1	49.0227	6.7040
400×300	1	1	1	130.9464	17.5922
500×400	1	1	1	272.1105	36.3245
600×500	1	1	1	453.2466	59.3510

Table 2. The comparison of calculation efficiency for equivalent resistance formulas (4.2) and (5.2).

$m \times n$	r	r_0	r_1	t_1	t_2
100×80	1	1	1	2.1134	0.3025
200×100	1	1	1	10.3649	1.4459
300×200	1	1	1	47.3364	6.3218
400×300	1	1	1	124.0385	16.6283
500×400	1	1	1	258.6759	34.3150
600×500	1	1	1	429.6586	56.1510

Table 3. The comparison of calculation efficiency for equivalent resistance formulas (4.3) and (5.3).

$m \times n$	r	r_0	r_1	t_1	t_2
100×80	1	1	1	2.0686	0.3154
200×100	1	1	1	10.3438	1.5022
300×200	1	1	1	46.6202	6.5125
400×300	1	1	1	123.0294	17.0670
500×400	1	1	1	255.7654	35.0518
600×500	1	1	1	424.8610	56.9760

Tables 1–3 demonstrate the comparison of calculation efficiency between the three original formulas and the optimized formulas when $d_1 = (0, 0)$, $r = r_0 = r_1 = 1$, under different resistor network scales.

Table 4. The comparison of calculation efficiency for equivalent resistance formulas (4.1) and (5.1).

$m \times n$	r	r_0	r_1	t_1	t_2
300×200	0.1	1	1	46.1489	6.3012
400×300	0.1	1	1	124.1933	16.4533
500×400	0.1	1	1	258.9349	33.7327
600×600	0.1	1	1	559.4526	71.8150
700×700	0.1	1	1	888.4606	113.1800
1000×1000	0.1	1	1	–	327.3041

Table 5. The comparison of calculation efficiency for equivalent resistance formulas (4.2) and (5.2).

$m \times n$	r	r_0	r_1	t_1	t_2
300×200	0.1	1	1	46.5638	6.3750
400×300	0.1	1	1	124.1012	16.5507
500×400	0.1	1	1	257.9374	33.9606
600×600	0.1	1	1	558.7647	71.7020
700×700	0.1	1	1	880.1761	111.6293
1000×1000	0.1	1	1	–	322.4906

Table 6. The comparison of calculation efficiency for equivalent resistance formulas (4.3) and (5.3).

$m \times n$	r	r_0	r_1	t_1	t_2
300×200	0.1	1	1	45.8709	6.5736
400×300	0.1	1	1	121.8801	16.8996
500×400	0.1	1	1	255.0192	34.5999
600×600	0.1	1	1	547.2879	74.3344
700×700	0.1	1	1	872.2106	114.7769
1000×1000	0.1	1	1	–	348.4239

Table 7. The comparison of calculation efficiency for equivalent resistance formulas (4.1) and (5.1).

$m \times n$	r	r_0	r_1	t_1	t_2
400×300	1	0.1	1	102.5669	13.3473
500×400	1	0.1	1	198.1812	26.8643
600×500	1	0.1	1	340.6793	46.0543
700×700	1	0.1	1	632.4905	84.0681
800×800	1	0.1	1	920.5850	123.0619
1000×1000	1	0.1	1	–	234.9719

Table 8. The comparison of calculation efficiency for equivalent resistance formulas (4.2) and (5.2).

$m \times n$	r	r_0	r_1	t_1	t_2
400×300	1	0.1	1	101.5474	13.7645
500×400	1	0.1	1	196.7793	26.6959
600×500	1	0.1	1	344.8172	45.6919
700×700	1	0.1	1	623.8246	82.6657
800×800	1	0.1	1	916.8383	121.4126
1000×1000	1	0.1	1	–	228.7297

Table 9. The comparison of calculation efficiency for equivalent resistance formulas (4.3) and (5.3).

$m \times n$	r	r_0	r_1	t_1	t_2
400×300	1	0.1	1	101.6689	14.2586
500×400	1	0.1	1	196.6264	27.6493
600×500	1	0.1	1	344.2061	45.6482
700×700	1	0.1	1	625.0337	83.5090
800×800	1	0.1	1	916.8602	122.5768
1000×1000	1	0.1	1	–	230.7143

Table 10. The comparison of calculation efficiency for equivalent resistance formulas (4.1) and (5.1).

$m \times n$	r	r_0	r_1	t_1	t_2
400×300	1	1	0.1	124.0123	16.6234
500×400	1	1	0.1	258.9065	34.1610
600×600	1	1	0.1	491.2254	64.3837
700×700	1	1	0.1	752.0369	99.3462
1000×1000	1	1	0.1	–	268.8378
1500×1500	1	1	0.1	–	844.9737

Table 11. The comparison of calculation efficiency for equivalent resistance formulas (4.2) and (5.2).

$m \times n$	r	r_0	r_1	t_1	t_2
400×300	1	1	0.1	122.7504	16.4076
500×400	1	1	0.1	253.9374	33.9152
600×600	1	1	0.1	485.4244	63.0957
700×700	1	1	0.1	743.9324	97.0477
1000×1000	1	1	0.1	–	263.8606
1500×1500	1	1	0.1	–	833.5678

Table 12. The comparison of calculation efficiency for equivalent resistance formulas (4.3) and (5.3).

$m \times n$	r	r_0	r_1	t_1	t_2
400×300	1	1	0.1	123.5598	16.8619
500×400	1	1	0.1	255.0641	34.9176
600×600	1	1	0.1	483.3796	64.6518
700×700	1	1	0.1	740.9571	99.2226
1000×1000	1	1	0.1	–	269.2752
1500×1500	1	1	0.1	–	850.4470

Tables 4–12 demonstrate the comparison of calculation efficiency between the three original formulas and the optimized formulas under different resistor network scales, when $d_1 = (0, 0)$, r, r_0, and r_1 take on different resistance values.

Table 13. The comparison of calculation efficiency for equivalent resistance formulas (4.1) and (5.1).

d_1	r	r_0	r_1	t_1	t_2
$(0, 0)$	1	1	1	287.2009	39.0213
$(100, 100)$	1	1	1	331.0542	43.5153
$(200, 200)$	1	1	1	330.9252	43.8494
$(300, 300)$	1	1	1	333.9882	43.6171
$(400, 400)$	1	1	1	331.8870	43.5418
$(500, 500)$	1	1	1	291.8674	40.0112

Table 14. The comparison of calculation efficiency for equivalent resistance formulas (4.2) and (5.2).

d_1	r	r_0	r_1	t_1	t_2
$(0, 0)$	1	1	1	283.1312	38.9512
$(100, 100)$	1	1	1	330.7856	43.1121
$(200, 200)$	1	1	1	331.2546	42.7238
$(300, 300)$	1	1	1	332.0763	42.9871
$(400, 400)$	1	1	1	331.0865	43.0201
$(500, 500)$	1	1	1	288.7652	39.4102

Table 15. The comparison of calculation efficiency for equivalent resistance formulas (4.3) and (5.3).

d_1	r	r_0	r_1	t_1	t_2
$(0, 0)$	1	1	1	290.0054	38.0398
$(100, 100)$	1	1	1	331.4275	43.8749
$(200, 200)$	1	1	1	335.0756	44.1664
$(300, 300)$	1	1	1	334.2624	44.0014
$(400, 400)$	1	1	1	333.1217	43.7522
$(500, 500)$	1	1	1	290.9776	40.1867

Tables 13–15 demonstrate the comparison of calculation efficiency between the three original formulas and the optimized formulas when the resistor network scale is 500×500 and $r = r_0 = r_1 = 1$, with d_1 at different positions on the resistor network.

Table 16. The comparison of calculation efficiency for equivalent resistance formulas (4.1) and (5.1).

$m \times n$	r	r_0	r_1	t_1	t_2
500×500	1	100	1	311.4661	42.2254
500×500	1	10	1	311.0778	41.6979
500×500	1	1	1	286.9392	38.8447
500×500	1	0.1	1	238.5423	33.3052
500×500	1	0.01	1	215.9418	30.6747
500×500	1	0.001	1	206.5932	29.5556

Table 17. The comparison of calculation efficiency for equivalent resistance formulas (4.2) and (5.2).

$m \times n$	r	r_0	r_1	t_1	t_2
500×500	1	100	1	313.0235	41.4472
500×500	1	10	1	312.3204	40.5223
500×500	1	1	1	295.7632	38.5525
500×500	1	0.1	1	239.6477	32.0898
500×500	1	0.01	1	218.5301	29.7269
500×500	1	0.001	1	210.2919	27.8761

Table 18. The comparison of calculation efficiency for equivalent resistance formulas (4.3) and (5.3).

$m \times n$	r	r_0	r_1	t_1	t_2
500×500	1	100	1	313.0125	42.9886
500×500	1	10	1	311.9131	41.3279
500×500	1	1	1	295.7632	39.0744
500×500	1	0.1	1	239.5199	32.8809
500×500	1	0.01	1	219.7493	29.6860
500×500	1	0.001	1	206.0903	27.9331

Tables 16–18 demonstrate the comparison of calculation efficiency between the three original formulas and the optimized formulas when the scale of resistor network is consistent, $d_1 = (0, 0)$, $r = r_1 = 1$, and r_0 takes on different resistance values.

Remark 3: The experimental data from Tables 1–12 show that when the resistance values are the same and the selection of the fixed node d_1 is consistent, the CPU times required to calculate the equivalent resistance by Eqs (4.1)–(4.3) and Eqs (5.1)–(5.3) will gradually increase with the enlargement of

the resistor network scale. However, regardless of how the resistor network scale changes, under the same conditions, the calculation efficiency of the optimized Eqs (5.1)–(5.3) is approximately 7 times higher than that of the original Eqs (4.1)–(4.3). From Tables 4 to 12, it can be observed that When the scale of the resistor network reaches 1000×1000, the original formulas have become very difficult to compute, while the optimized formulas can still complete the calculation tasks very quickly. This further demonstrates the necessity of the optimized formulas (5.1), (5.2) and (5.3).

Remark 4: The experimental data from Tables 13–15 can be observed to show that under the same resistor network scale and conditions, the calculation efficiency of both the original formulas and the optimized formulas does not change significantly. However, comparatively, if the selection point d_1 is at the edge of the resistor network, the CPU times cost to calculate the equivalent resistance is relatively less.

Remark 5: The experimental data from Tables 1–12 show that reducing the resistance value of r_0 can improve the calculation efficiency of both the original and optimized formulas to a certain extent. The experimental data from Tables 16–18 further suggest that as the resistance value of r_0 decreases, the computational efficiency of both the original and optimized formulas will be enhanced to some degree when processing resistor networks of the same scale. However, this improvement in computational efficiency will cease when the resistance value of r_0 becomes sufficiently small.

9. Conclusions

In this paper, we propose a heuristic path planning algorithm based on the potential function and successfully apply it to the globe model. This method ingeniously utilizes the characteristic that the potential in the resistor network decreases gradiently from the current input point to the current output point. It provides a new perspective for the design of path planning algorithms and pioneers new applications for resistor networks. By introducing the Chebyshev polynomial of the second class, the original equivalent resistance formulas are optimized, significantly improving the computational efficiency of equivalent resistance. This offers an effective method for dealing with large-scale data issues. We used several specific examples to plot corresponding three-dimensional views, demonstrating the changes in equivalent resistance between two points under different conditions. The final comparative experiments confirmed that the optimized equivalent resistance formulas can save a considerable amount of time cost when processing large-scale resistor networks compared to the original formulas.

Use of AI tools declaration

The authors declare they have not used Artificial Intelligence (AI) tools in the creation of this article.

Acknowledgments

The research was supported by the National Natural Science Foundation of China (Grant No.12101284), the Natural Science Foundation of Shandong Province (Grant No. ZR2022MA092) and the Department of Education of Shandong Province (Grant No.2023KJ214).

Conflict of interest

The authors declare there is no conflicts of interest.

References

1. Z. Tan, Recursion-transform method to a non-regular $m \times n$ cobweb with an arbitrary longitude, *Sci. Rep.*, **5** (2015), 11266. https://doi.org/10.1038/srep11266
2. M. Darwish, H. Boysan, C. Liewald, B. Nickel, A. Gagliardi, A resistor network simulation model for laser-scanning photo-current microscopy to quantify low conductance regions in organic thin films, *Org. Electron.*, **62** (2018), 474–480. https://doi.org/10.1016/j.orgel.2018.08.002
3. G. Xu, G. V. Eleftheriades, S. V. Hum, Analysis and design of general printed circuit board metagratings with an equivalent circuit model approach, *IEEE Trans. Antennas Propag.*, **69** (2021), 4657–4669. https://doi.org/10.1109/TAP.2021.3060084
4. P. Willke, T. Kotzott, T. Pruschke, M. Wenderoth, Magnetotransport on the nano scale, *Nat. Commun.*, **8** (2017), 15283. https://doi.org/10.1038/ncomms15283
5. Y. Hadad, J. C. Soric, A. B. Khanikaev, A. Alù, Self-induced topological protection in nonlinear circuit arrays, *Nat. Electron.*, **1** (2018), 178–182. https://doi.org/10.1038/s41928-018-0042-z
6. D. Zhang, B. Yang, J. Tan, Y. Jin, B. Xiao, G. Xian, et al., Impact damage localization and mode identification of CFRPs panels using an electric resistance change method, *Compos. Struct.*, **276** (2021), 114587. https://doi.org/10.1016/j.compstruct.2021.114587
7. K. Rhazaoui, Q. Cai, C. S. Adjiman, N. P. Brandon, Towards the 3D modeling of the effective conductivity of solid oxide fuel cell electrodes: I. Model development, *Chem. Eng. Sci.*, **99** (2013), 161–170. https://doi.org/10.1016/j.ces.2013.05.030
8. Z. Zhu, Y. Yin, H. Lyu, Automatic collision avoidance algorithm based on route-plan-guided artificial potential field method, *Ocean Eng.*, **271** (2023), 113737. https://doi.org/10.1016/j.oceaneng.2023.113737
9. Y. Ji, L. Ni, C. Zhao, C. Lei, Y. Du, W. Wang, TriPField: A 3D potential field model and its applications to local path planning of autonomous vehicles, *IEEE Trans. Intell. Transp. Syst.*, **24** (2023), 3541–3554. https://doi.org/10.1109/TITS.2022.3231259
10. Z. Yu, J. Yuan, Y. Li, C. Yuan, S. Deng, A path planning algorithm for mobile robot based on water flow potential field method and beetle antennae search algorithm, *Comput. Electr. Eng.*, **109** (2023), 108730. https://doi.org/10.1016/j.compeleceng.2023.108730
11. C. Mahulea, M. Kloetzer, R. González, *Path Planning of Cooperative Mobile Robots Using Discrete Event Models*, 1st edition, John Wiley & Sons, 2020. https://doi.org/10.1002/9781119486305
12. J. Xue, J. Li, J. Chen, C. Tu, A. Stancu, X. Wang, Wall-climbing robot path planning for cylindrical storage tank inspection based on modified A-star algorithm, in *2021 IEEE Far East NDT New Technology & Application Forum (FENDT)*, (2021), 191–195. https://doi.org/10.1109/FENDT54151.2021.9749634

13. A. UĞUR, Path planning on a cuboid using genetic algorithms, *Inf. Sci.*, **178** (2008), 113737. https://doi.org/10.1016/j.ins.2008.04.005

14. G. Kulathunga, A reinforcement learning based path planning approach in 3D environment, *Procedia Comput. Sci.*, **212** (2022), 152–160. https://doi.org/10.1016/j.procs.2022.10.217

15. H. Mazaheri, S. Goli, A. Nourollah, Path planning in three-dimensional space based on butterfly optimization algorithm, *Sci. Rep.*, **14** (2024), 2332. https://doi.org/10.1038/s41598-024-52750-9

16. G. Kirchhoff, Ueber die Auflösung der Gleichungen, auf welche man bei der Untersuchung der linearen Vertheilung galvanischer Ströme geführt wird, *Ann. Phys.-Berlin*, **148** (1847), 497–508. https://doi.org/10.1002/andp.18471481202

17. C. Pennetta, E. Alfinito, L. Reggiani, F. Fantini, I. DeMunari, A. Scorzoni, Biased resistor network model for electromigration failure and related phenomena in metallic lines, *Phys. Rev. B*, **70** (2004), 174305. https://link.aps.org/doi/10.1103/PhysRevB.70.174305

18. M. Lai, W. Wang, Fast direct solvers for Poisson equation on 2D polar and spherical geometries, *Numer. Methods Partial Differ. Equations*, **18** (2002), 56–68. https://doi.org/10.1002/num.1038

19. V. Winstead, C. L. DeMarco, Network essentiality, *IEEE Trans. Circuits Syst. I Regul. Pap.*, **60** (2012), 703–709. https://doi.org/10.1109/TCSI.2012.2215734

20. G. Ferri, G. Antonini, Ladder-network-based model for interconnects and transmission lines time delay and cutoff frequency determination, *J. Circuit. Syst. Comput.*, **16** (2007), 489–505. https://doi.org/10.1142/S0218126607003794

21. M. Q. Owaidat, R. S. Hijjawi, J. M. Khalifeh, Network with two extra interstitial resistors, *Int. J. Theor. Phys.*, **51** (2012), 3152–3159. https://doi.org/10.1007/s10773-012-1196-5

22. N. S. Izmailian, M. Huang, Asymptotic expansion for the resistance between two maximally separated nodes on an M by N resistor network, *Phys. Rev. E*, **82** (2010), 011125. https://doi.org/10.1103/PhysRevE.82.011125

23. D. J. Klein, M. Randić, Resistance distance, *J. Math. Chem.*, **12** (1993), 81–95. https://doi.org/10.1007/BF01164627

24. Y. Yang, D. J. Klein, A recursion formula for resistance distances and its applications, *Discrete Appl. Math.*, **161** (2013), 2702–2715. https://doi.org/10.1016/j.dam.2012.07.015

25. D. J. Klein, Centrality measure in graphs, *J. Math. Chem.*, **47** (2010), 1209–1223. https://doi.org/10.1007/s10910-009-9635-0

26. N. Chair, The effective resistance of the N-cycle graph with four nearest neighbors, *J. Stat. Phys.*, **154** (2014), 1177–1190. https://doi.org/10.1007/s10955-014-0916-z

27. H. Chen, F. Zhang, Resistance distance local rules, *J. Math. Chem.*, **44** (2008), 405–417. https://doi.org/10.1007/s10910-007-9317-8

28. S. Katsura, S. Inawashiro, Lattice Green's functions for the rectangular and the square lattices at arbitrary points, *J. Math. Phys.*, **12** (1971), 1622–1630. https://doi.org/10.1063/1.1665785

29. W. Kook, Combinatorial Green's function of a graph and applications to networks, *Adv. Appl. Math.*, **46** (2011), 417–423. https://doi.org/10.1016/j.aam.2010.10.006

30. J. Cserti, Application of the lattice Green's function for calculating the resistance of an infinite network of resistors, *Am. J. Phys.*, **68** (2000), 896–906. https://doi.org/10.1119/1.1285881

31. S. Giordano, Disordered lattice networks: general theory and simulations, *Int. J. Circuit Theory Appl.*, **33** (2005), 519–540. https://doi.org/10.1002/cta.335

32. S. Kirkpatrick, Percolation and conduction, *Rev. Mod. Phys.*, **45** (1973), 574. https://link.aps.org/doi/10.1103/RevModPhys.45.574

33. L. Borges, P. Daripa, A fast parallel algorithm for the Poisson equation on a disk, *J. Comput. Phys.*, **169** (2001), 151–192. https://doi.org/10.1006/jcph.2001.6720

34. N. Chair, Trigonometrical sums connected with the chiral Potts model, Verlinde dimension formula, two-dimensional resistor network, and number theory, *Ann. Phys.*, **314** (2014), 56–76. https://doi.org/10.1016/j.aop.2013.11.012

35. F. Y. Wu, Theory of resistor networks: the two-point resistance, *J. Phys. A: Math. Gen.*, **37** (2004), 6653. https://doi.org/10.1088/0305-4470/37/26/004

36. W. J. Tzeng, F. Y. Wu, Theory of impedance networks: the two-point impedance and *LC* resonances, *J. Phys. A: Math. Gen.*, **39** (2006), 8579. https://doi.org/10.1088/0305-4470/39/27/002

37. J. W. Essam, F. Y. Wu, The exact evaluation of the corner-to-corner resistance of an $M \times N$ resistor network: asymptotic expansion, *J. Phys. A: Math. Theor.*, **42** (2008), 025205. https://doi.org/10.1088/1751-8113/42/2/025205

38. N. S. Izmailian, R. Kenna, F. Y. Wu, The two-point resistance of a resistor network: a new formulation and application to the cobweb network, *J. Phys. A: Math. Theor.*, **47** (2013), 035003. https://doi.org/10.1088/1751-8113/47/3/035003

39. N. S. Izmailian, R. Kenna, A generalised formulation of the Laplacian approach to resistor networks, *J. Stat. Mech.: Theory Exp.*, **9** (2014), 09016. https://doi.org/10.1088/1742-5468/2014/09/P09016

40. Z. Tan, J. W. Essam, F. Y. Wu, Two-point resistance of a resistor network embedded on a globe, *Phys. Rev. E*, **90** (2014), 012130. https://doi.org/10.1103/PhysRevE.90.012130

41. Z. Tan, Z. Tan, Electrical properties of an $m \times n$ rectangular network, *Phys. Scr.*, **95** (2020), 035226. https://doi.org/10.1088/1402-4896/ab5977

42. Z. Tan, Z. Tan, Electrical properties of $m \times n$ cylindrical network, *Chin. Phys. B*, **29** (2020), 080503. https://doi.org/10.1088/1674-1056/ab96a7

43. Z. Tan, Resistance theory for two classes of n-periodic networks, *Eur. Phys. J. Plus*, **137** (2022), 1–12. https://doi.org/10.1140/epjp/s13360-022-02750-3

44. Z. Tan, Z. Tan, J. Chen, Potential formula of the nonregular $m \times n$ fan network and its application, *Sci. Rep.*, **8** (2018), 5798. https://doi.org/10.1038/s41598-018-24164-x

45. Z. Tan, Theory of an $m \times n$ apple surface network with special boundary, *Commun. Theor. Phys.*, **75** (2023), 065701. https://doi.org/10.1088/1572-9494/accb82

46. Z. Tan, Electrical property of an $m \times n$ apple surface network, *Results Phys.*, **47** (2023), 106361. https://doi.org/10.1016/j.rinp.2023.106361

47. Z. Tan, Z. Tan, Potential formula of an $m \times n$ globe network and its application, *Sci. Rep.*, **8** (2018), 9937. https://doi.org/10.1038/s41598-018-27402-4

48. S. Zhou, Z. Wang, Y. Zhao, Z. Tan, Electrical properties of a generalized $2 \times n$ resistor network, *Commun. Theor. Phys.*, **75** (2023), 075701. https://doi.org/10.1088/1572-9494/acd2b9

49. Y. Wei, X. Jiang, Z. Jiang, S. Shon, Determinants and inverses of perturbed periodic tridiagonal Toeplitz matrices, *Adv. Differ. Equ.*, **2019** (2019), 410. https://doi.org/10.1186/s13662-019-2335-6

50. Y. Wei, Y. Zheng, Z. Jiang, S. Shon, A study of determinants and inverses for periodic tridiagonal Toeplitz matrices with perturbed corners involving Mersenne numbers, *Mathematics*, **7** (2019), 893. https://doi.org/10.3390/math7100893

51. J. Wang, Y. Zheng, Z. Jiang, Norm equalities and inequalities for tridiagonal perturbed Toeplitz operator matrIices, *J. Appl. Anal. Comput.*, **13** (2023), 671–683. https://doi.org/10.11948/20210489

52. Y. Wei, X. Jiang, Z. Jiang, S. Shon, On inverses and eigenpairs of periodic tridiagonal Toeplitz matrices with perturbed corners, *J. Appl. Anal. Comput.*, **10** (2020), 178–191. https://doi.org/10.11948/20190105

53. Y. Fu, X. Jiang, Z. Jiang, S. Jhang, Properties of a class of perturbed Toeplitz periodic tridiagonal matrices, *Comp . Appl. Math.*, **57** (2020), 1–19. https://doi.org/10.1007/s40314-020-01171-1

54. Y. Fu, X. Jiang, Z. Jiang, S. Jhang, Inverses and eigenpairs of tridiagonal Toeplitz matrix with opposite-bordered rows, *J. Appl. Anal. Comput.*, **10** (2020), 1599–1613. https://doi.org/10.11948/20190287

55. Y. Wei, Y. Zheng, Z. Jiang, S. Shon, The inverses and eigenpairs of tridiagonal Toeplitz matrices with perturbed rows, *J. Appl. Math. Comput.*, **68** (2022), 623–636. https://doi.org/10.1007/s12190-021-01532-x

56. Z. Jiang, W. Wang, Y. Zheng, B. Zuo, B. Niu, Interesting explicit expressions of determinants and inverse matrices for Foeplitz and Loeplitz Matrices, *Mathematics*, **7** (2019), 939. https://doi.org/10.3390/math7100939

57. Q. Meng, Y. Zheng, Z. Jiang, Exact determinants and inverses of (2,3,3)-Loeplitz and (2,3,3)-Foeplitz matrices., *Comp. Appl. Math.*, **41** (2022), 35. https://doi.org/10.1007/s40314-021-01738-6

58. Q. Meng, Y. Zheng, Z. Jiang, Determinants and inverses of weighted Loeplitz and weighted Foeplitz matrices and their applications in data encryption, *J. Appl. Math. Comput.*, **68** (2022), 3999–4015. https://doi.org/10.1007/s12190-022-01700-7

59. Q. Meng, X. Zheng, Z. Jiang, Interesting determinants and inverses of skew Loeplitz and Foeplitz matrices, *J. Appl. Anal. Comput.*, **11** (2021), 2947–2958. https://doi.org/10.11948/20210070

60. Y. Shi, L. Jin, S. Li, J. Li, J. Qiang, D. K. Gerontitis, Novel discrete-time recurrent neural networks handling discrete-form time-variant multi-augmented Sylvester matrix problems and manipulator application, *IEEE Trans. Neural Networks Learn. Syst.*, **33** (2020), 587–599. https://doi.org/10.1109/TNNLS.2020.3028136

61. Z. Sun, G. Wang, L. Jin, C. Cheng, B. Zhang, J. Yu, Noise-suppressing zeroing neural network for online solving time-varying matrix square roots problems: A control-theoretic approach, *Expert Syst. Appl.*, **192** (2022), 116272. https://doi.org/10.1016/j.eswa.2021.116272
62. L. Jin, Y. Qi, X. Luo, S. Li, M. Shang, Distributed competition of multi-robot coordination under variable and switching topologies, *IEEE Trans. Autom. Sci. Eng.*, **19** (2021), 3575–3586. https://doi.org/10.1109/TASE.2021.3126385
63. L. Jin, X. Zheng, X. Luo, Neural dynamics for distributed collaborative control of manipulators with time delays, *IEEE/CAA J. Autom. Sin.*, **9** (2022), 854–863. https://doi.org/10.1109/JAS.2022.105446
64. X. Wang, M. Che, Y. Wei, Complex-valued neural networks for the Takagi vector of complex symmetric matrices, *Neurocomputing*, **223** (2017), 77–85. https://doi.org/10.1016/j.neucom.2016.10.034
65. W. Wu, Y. Zhang, Zeroing neural network with coefficient functions and adjustable parameters for solving time-variant Sylvester equation, *IEEE Trans. Neural Networks Learn. Syst.*, **35** (2022), 6757–6766. https://doi.org/10.1109/TNNLS.2022.3212869
66. Q. Hu, B. Zheng, An efficient Takagi-Sugeno fuzzy zeroing neural network for solving time-varying Sylvester equation, *IEEE Trans. Fuzzy Syst.*, **31** (2022), 2401–2411. https://doi.org/10.1109/TFUZZ.2022.3225630
67. X. Jiang, G. Zhang, Y. Zheng, Z. Jiang, Explicit potential function and fast algorithm for computing potentials in $\alpha \times \beta$ conic surface resistor network, *Expert Syst. Appl.*, **238** (2024), 122–157. https://doi.org/10.1016/j.eswa.2023.122157
68. Y. Zhou, Y. Zheng, X. Jiang, Z. Jiang, Fast algorithm and new potential formula represented by Chebyshev polynomials for an $m \times n$ globe network, *Sci. Rep.*, **12** (2022), 21260. https://doi.org/10.1038/s41598-022-25724-y
69. Z. Jiang, Y. Zhou, X. Jiang, Y. Zheng, Analytical potential formulae and fast algorithm for a horn torus resistor network, *Phys. Rev. E*, **107** (2023), 044123. https://doi.org/10.1103/PhysRevE.107.044123
70. X. Meng, X. Jiang, Y. Zheng, Z. Jiang, A novel formula for representing the equivalent resistance of the $m \times n$ cylindrical resistor network, *Sci. Rep.*, **14** (2024), 21254. https://doi.org/10.1038/s41598-024-72196-3
71. G. Udrea, A note on the sequence $(W_n)_{n\geq 0}$ of A. F. Horadam, *Port. Math.*, **53** (1996), 143–156.
72. J. C. Mason, D. C. Handscomb, *Chebyshev Polynomials*, 1st edition, Chapman and Hall/CRC, 2002.

AIMS Press